

國立臺灣大學電機資訊學院電信工程研究所

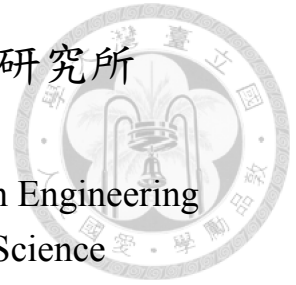
碩士論文

Graduate Institute of Computer Science and Information Engineering

College of Electrical Engineering and Computer Science

National Taiwan University

Master Thesis



擴散式分子通訊下之調變設計

Modulation Design in Diffusion-based Molecular Communication
System

林維安

Wei-An Lin

指導教授：葉丙成 博士

Advisor: Ping-Cheng Yeh, Ph.D.

中華民國 103 年 7 月

July, 2014

國立臺灣大學 (碩) 博士學位論文

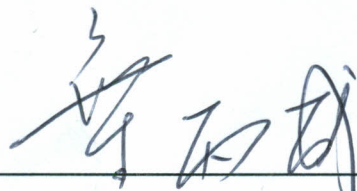
口試委員會審定書

擴散式分子通訊下之調變設計

Modulation Design in Diffusion-based Molecular
Communication System

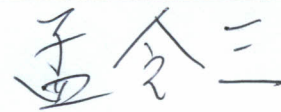
本論文係林維安君 (學號 R01942045) 在國立臺灣大學電信工程學研究所完成之碩 (博) 士學位論文，於民國 103 年 7 月 16 日承下列考試委員審查通過及口試及格，特此證明

口試委員：



(簽名)


(指導教授)



所 長

(簽名)

誌謝



在電信所碩士的生活即將畫下句點。這兩年中我學到很多，許多想法也與當初大學畢業的我不同了。首先要感謝指導教授葉丙成老師。感謝老師從大學部專題以來的照顧，不僅是研究上給予我們意見，對我們成長、學習也相當關心。其中印象最深刻的是老師開的簡報課，讓我對上台口頭報告不再那麼害怕，即使是到國外參加 conference，我都有足夠信心向聽眾表達我的想法。另外，老師推薦我們修 Stanford 線上學術寫作課程，實在令我收穫良多。從這門課，我學到即使沒有寫曠世奇作的才華，只要抓住寫作的幾個小技巧，也能讓日常寫作甚至論文寫作相當生動且有條理。修過這門課後，我變得對寫文章更有自信，在碩二考 GRE 寫作時拿到高分。這都得歸功於老師對我們學習上的關心！另外我要謝謝彥奇學長引導我接觸數學的領域。仍記得大學時期一直排斥接觸分析數學，直到彥奇學長的「推坑」，我在研究所一年級上學期，一邊惡補高微一邊修實分析，改變了我對數學的看法。之後更開啟我對數學的興趣，甚至讓我能以不同的角度理解不同領域的研究，令我獲益良多。謝謝實驗室的同學們，這一屆的博理 515 實在是超棒的！大家一起到處玩、一起討論研究、一起聊天，令我度過相當精彩且快樂的碩士生活。偉軒、圈圈、穴宇、李俊，很高興能與你們在同一個實驗室相處兩年！當然也要感謝分子通訊小組的學弟們。駿挺的見解與研究給我更多的想法，使我能將現有的題材延伸。昀鋒常常和我討論數學的分析，幫我突破許多難關，真的非常感謝。博凱常對我的研究內容提出不同觀點，使我能檢討以前做過的題目。還記得碩一時和博凱一起研究 synchronization，結果我因為做其他題目而放博凱鳥，實在不好意思…不過後來博凱還是靠自己做出相當棒的成果！（好加在 XD）最後要感謝我的爸媽，沒有他們我絕對無法進碩士念書，他們的支持給我很大的幫助，希望你們永遠身體健康、快快樂樂。

差點忘了，我還要感謝上帝，thank God！因為要感謝的人太多，只好謝天了。

摘要



在奈米尺度的通訊環境下，擴散式分子通訊被視為最可行也最具潛力的方法。近期對於擴散式分子通訊調變的研究包含利用分子種類、分子數量以及分子濃度來承載訊息。本篇碩士論文依照承載訊息、偵測方法的差異，將擴散式分子通訊分為兩大類：同調分子通訊以及非同調分子通訊，藉此研究並設計分子通訊系統。對於同調分子通訊，我們研究利用分子數量以及分子種類承載訊息。由於擴散通道的隨機性，錯位效應（cross over effect）以及符際干擾（inter-symbol interference）嚴重影響系統效能。本篇論文提出符際干擾消除（ISI cancellation）以及閾值偵測法（threshold-based detection）來消除上述對於系統的負面效應。經由數學分析以及電腦模擬證實，本篇論文針對通道負面效應所提出的數量-種類調變（quantity-type modulation）能有效提升系統效能。對於非同調分子通訊，本論文建構了統計模型，以數學描述接收端偵測到的濃度變化。由於此模型適用於傳送端發出任意連續波型，能設計出的調變方法會更加豐富，同時也利於設計更好的偵測演算法。另外，本論文提出基底展開偵測法（expansion-based detection）和廣泛被使用的取樣偵測法（sample-based detection）做比較，電腦模擬結果顯示基底展開偵測法在振幅調變以及脈衝位置調變下能比取樣偵測法達到更佳系統效能。

ABSTRACT



Diffusion-based molecular communication has become a promising scheme for communication between nanoscale devices, and various modulation schemes have recently been proposed, including type, quantity, and concentration modulation. In this thesis, we investigate molecular communication by separating it into two categories: coherent molecular communication and non-coherent molecular communication, which are based on the adopted signaling and detection methods. For coherent molecular communication, we study modulations that convey information in molecular quantity or molecular type. Due to the randomness of each molecule in the diffusion channel, problems such as the crossover effect and the inter-symbol interference arise which undermine the system performance. This thesis provides algorithms such as ISI cancellation and threshold-based detection algorithm to deal with the problems. Moreover, it is shown by mathematical derivations and computer simulations that the proposed quantity-type modulation, which is designed against the bad channel effects, has reliable performance. For non-coherent molecular communication, we construct a stochastic model to describe the concentration magnitude sensed by the receiver. The model enables more modulation designs since it is generalized to the case that the transmitter send any continuous wave to the the receiver. It also allows better design for detection algorithm. Amplitude modulation and pulse-position modulation in non-coherent molecular communication are studied and compared by using the proposed expansion-based detection as well as the widely-used sampling-based detection. Through simulation, it is proved that the expansion-based detection outperforms the sampling-based detection.

TABLE OF CONTENTS



ABSTRACT	ii
LIST OF FIGURES	v
CHAPTER 1 INTRODUCTION	1
1.1 Overview	1
1.2 Coherent Molecular Communication	2
1.3 Non-coherent Molecular Communication	4
1.4 Thesis Organization	4
CHAPTER 2 QUANTITY MODULATION	6
2.1 Introduction	6
2.2 System Model	7
2.2.1 Transmission Nano-machine	7
2.2.2 Reception Nano-machine	7
2.2.3 Channel	8
2.2.4 QM System	8
2.3 Detection in One-shot Transmission	9
2.3.1 Binary Detection	9
2.3.2 M-ary Detection	11
2.3.3 Error Rate Analysis	12
2.4 Serial Transmission and ISI Cancellation	13
2.5 Numerical Results	15
2.5.1 SER Comparison with and without ISI Cancellation	15
2.5.2 Performance Under Different Duration of Time Slot	17
CHAPTER 3 QUANTITY-TYPE MODULATION	18
3.1 Introduction	18
3.2 System Model	19
3.2.1 Quantity-type Modulation	19
3.2.2 ISI and Noise Effect on Quantity-type Modulation	19
3.3 Detection Algorithms	20

3.3.1	Majority-vote Detection	21
3.3.2	Threshold-based Detection	22
3.3.3	Trade-offs when Combating ISI and Noise Effect on Quantity-type Modulation	23
3.4	BER Analysis	25
3.4.1	Preliminaries	25
3.4.2	Analysis when Background Noise is Negligible	26
3.4.3	Analysis when Background Noise is not Negligible	30
3.4.4	Optimal Choice of Signaling Interval T_s for Threshold-based Detection	35
3.5	Numerical Results	36
3.5.1	Performance when Background Noise is Negligible	37
3.5.2	Performance when Background Noise is not Negligible	38
CHAPTER 4 WAVEFORM MODULATION		44
4.1	Introduction	44
4.2	System Model	44
4.2.1	Transmitter and Receiver Modeling	44
4.2.2	Diffusion Channel Modeling	45
4.3	Signal Modulation and Detection	49
4.4	Numerical Results	54
4.4.1	Amplitude Modulation	55
4.4.2	Pulse-position Modulation	58
CHAPTER 5 CONCLUSIONS AND FUTURE WORKS		61
5.1	Conclusions	61
5.2	Future Works	62
REFERENCES		63

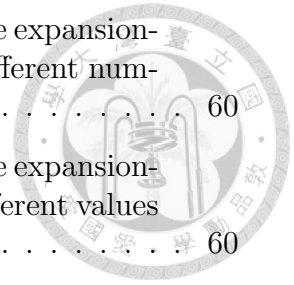
LIST OF FIGURES



1	Diffusion-based molecular communication.	2
2	Coherent molecular communication.	3
3	Transmission from TN to RN through a fluid medium.	7
4	Illustration of quantity-based modulation scheme with $L_0 = 2$, $L_1 = 4$, $L_2 = 6$, $L_3 = 8$	9
5	Demonstration of the process of finding η in a binary QM system, where f is the conditional PDF of N given H_m is true.	12
6	Theoretical result versus numerical result for one-shot binary quantity-based modulation.	13
7	Binary quantity-based modulation with ISI cancellation.	16
8	Quaternary quantity-based modulation with ISI cancellation.	16
9	Binary quantity-based modulation with ISI cancellation under different T_s	17
10	A demonstrative example for the majority-vote detection algorithm and the threshold-based detection algorithm with $\lambda = 1$ and $\lambda = 2$. The boxed numbers represent the value stored in the counter that reaches the threshold λ	20
11	Block diagram of the threshold-based detection algorithm.	21
12	A demonstrative example for the detection result under background noise using the threshold-based detection algorithm. $\lambda = 3$. In the example, the crossover effect is not taken into account.	24
13	Example of the events $\hat{E}_{001}^{\text{MVD}}$, $\hat{E}_{100}^{\text{MVD}}$, and $\hat{E}_{000}^{\text{MVD}}$ given that the information sequence '0, 1, 0' is transmitted.	29
14	Performance comparison between the majority-vote detection and the proposed threshold-based detection for the $n = 3$ quantity-type-modulated system without background noise. The theoretical analysis and the simulation results are also compared.	38
15	Performance comparison between the majority-vote detection and the proposed threshold-based detection for the $n = 5$ quantity-type-modulated system without background noise. The theoretical analysis and the simulation results are also compared.	39
16	Performance comparison of quantity-type-modulated systems without background noise with different n (the number of molecules released at a time) and different detection algorithms. The case of $n = 1$ corresponds to the type-modulated system. $\lambda = 1$ for the threshold-based detection algorithm.	40

17	Performance comparison between the majority-vote detection and the proposed threshold-based detection for the $n = 3$ quantity-type-modulated system with background noise. The theoretical analysis and the simulation results are also compared.	41
18	Performance comparison between the majority-vote detection and the proposed threshold-based detection for the $n = 5$ quantity-type-modulated system with background noise. The theoretical analysis and the simulation results are also compared.	41
19	Performance comparison between the majority-vote detection and the proposed threshold-based detection for the $n = 3$ quantity-type-modulated system with background noise under different block sizes. The theoretical analysis and the simulation results are also compared. $\lambda = 3$	42
20	Performance comparison between the majority-vote detection and the proposed threshold-based detection for the $n = 5$ quantity-type-modulated system with background noise under different block sizes. The theoretical analysis and the simulation results are also compared. $\lambda = 5$	42
21	Performance comparison of quantity-type-modulated systems with different n using different detection algorithms in the presence of background noise. The case of $n = 1$ corresponds to the type-modulated system. $\lambda = 3$ for the $n = 3$ quantity-type-modulated system and $\lambda = 5$ for the $n = 5$ quantity-type-modulated system. $L = 40$ bits.	43
22	Proposed diffusion model for molecular communication in a fluid medium.	46
23	Channel response results from an infinitesimal duration of transmitted signal $s(t)$	46
24	Patterns of the waveform $c_0(t)$ under different distance d and diffusion coefficient D . The time t is normalized with respect to T_s	56
25	Patterns of the waveform $c_0(t)$ under different symbol duration T_s . The time t is normalized with respect to T_s	56
26	Comparison between the sample-based detection and the expansion-based detection for the amplitude modulation under different values of diffusion coefficient D	57
27	Comparison between the sample-based detection and the expansion-based detection for amplitude modulation under different number of observations K	58
28	Comparison between the sample-based detection and the expansion-based detection for pulse-position modulation under different values of diffusion coefficient D	59

- 29 Comparison between the sample-based detection and the expansion-based detection for pulse-position modulation under different numbers of observations K 60
- 30 Comparison between the sample-based detection and the expansion-based detection for pulse-position modulation under different values of pulse width w 60



CHAPTER 1

INTRODUCTION



1.1 Overview

Nano-technology has become an important research area and is expected to have great impact on many fields, including medicine, biology, military, and electronics. The advance in nano-technology has enabled the development of nanomachines, which are devices in nanoscale that can perform sensing, computation, and actuation. The computational capability of a single nanomachine, however, is often quite limited due to the ultra-small size and the ultra-low power capacity. As a result, an efficient information exchange mechanism between nanomachines is required in order to coordinate the nanomachines to accomplish complicated tasks [1].

Unlike modern wireless communication systems in which signals are carried by electromagnetic (EM) waves, communication in nanoscale through EM waves may not be practical due to issues such as antenna size, power consumption, computational complexity, and signal attenuation in fluid environments [2]. Diffusion-based molecular communication is believed to be one of the most promising solutions for communication in nanoscale [3–7], which is composed of a transmission nanomachine (TN), a reception nano-machine (RN), and a diffusion channel between TN and RN. To convey information, TN releases information molecules into surrounding environment. Those molecules arrive at RN through diffusion process, RN then captures those arriving molecules and attains information. Fig. 1 shows a picture for diffusion-based molecular communication. This thesis focuses on designing modulation and detection schemes for TN to embed information and RN to attain information by molecules. To discuss modulation techniques thoroughly, we categorize diffusion-based molecular communication into two types –

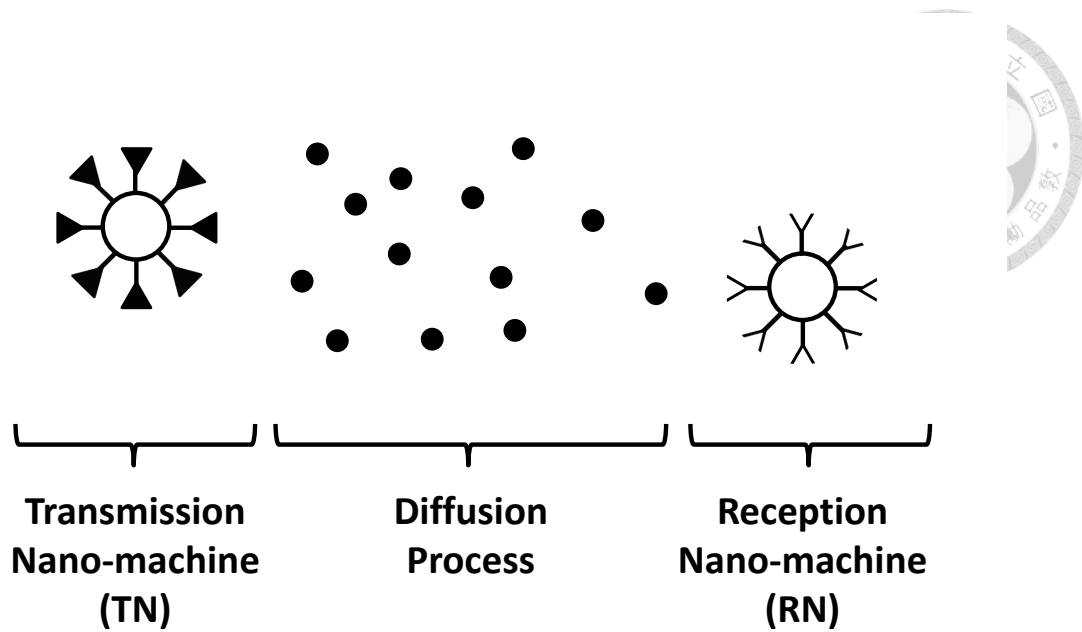


Figure 1: Diffusion-based molecular communication.

coherent or non-coherent molecular communication – according to the signaling and detection method used by TN and RN.

1.2 Coherent Molecular Communication

In communication based on EM wave, “coherent modulation” means receivers can fully recover phase of received signal. Borrowing the idea, we use the term *coherent* in molecular communication to mention RN can recover timing information of each molecule. In this thesis, *coherent molecular communication* means that the signaling and detection are done by counting the number of information molecules. Both TN and RN are able to count each molecule at a single position and time instant. Moreover, once an information molecule is captured by RN, it is removed from the diffusion channel. Diffusion model and channel capacity related to coherent molecular communication is first proposed in [8]. In coherent molecular communication, the behavior of each molecule can be investigated separately, in microscopic view. More precisely, for each molecule released by TN, we

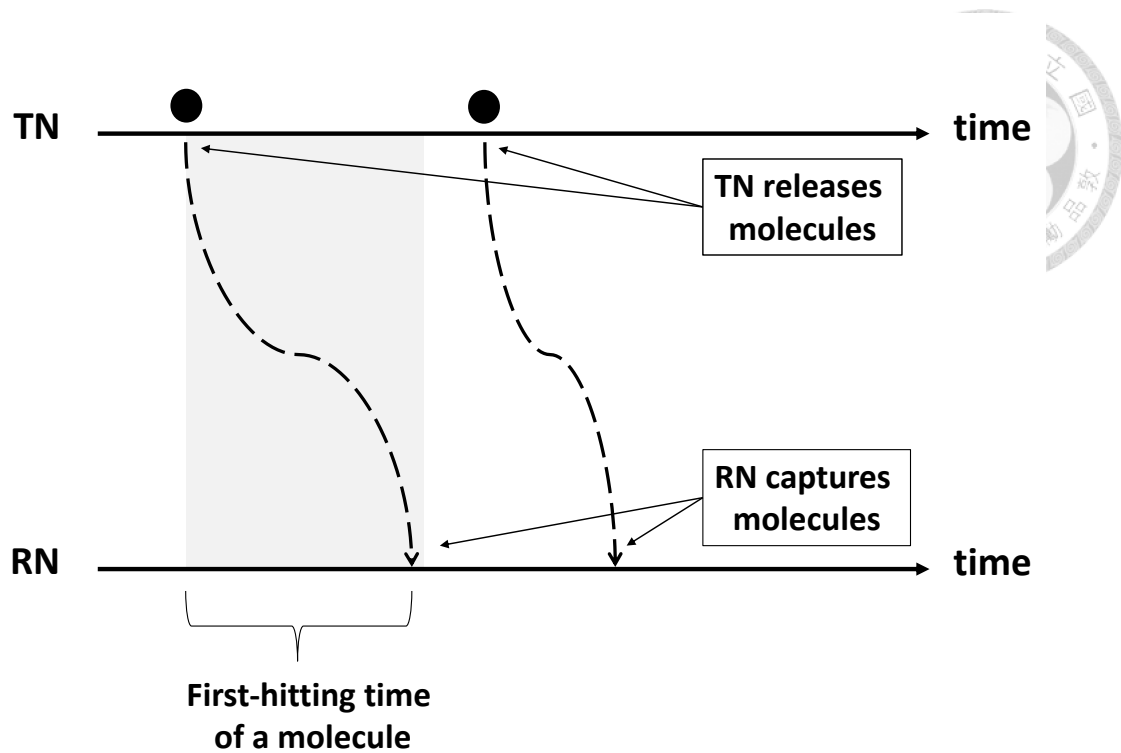


Figure 2: Coherent molecular communication.

can describe the behavior of this molecule by using the time it requires to reach RN, which we call the *first-hitting time* of a molecule. Fig. 2 shows an example for coherent molecular communication. One major issue in coherent molecular communication is that earlier released molecules may arrive late and later released molecules may arrive early, causing *crossovers*. When molecules are used to transmit symbols, crossovers between molecules will introduce interference. In this thesis, we investigate the problem known as *inter-symbol interference* (ISI) in coherent molecular communication, and propose two approaches to mitigate the effect. From simulation, we show that the proposed ISI cancellation algorithm can improve the performance significantly. Moreover, both the modulation and the detection methods have low complexity which are suitable for communication between nanomachines.

1.3 *Non-coherent Molecular Communication*

By *non-coherent molecular communication*, we mean the signaling and detection are done by sensing the magnitude of the molecular concentration, i.e. the number of molecules within a small volume around them, at a time instant. Noise model considering diffusion process and counting errors from ligand-binding imperfection is first proposed in [9]. In [10], information is modulated by pulses of molecules at transmission nano-machine (TN), and RN samples the received concentration waveform to make detection. [11, 12] study possible modulation techniques in molecular communication via different messenger molecules. Most of the existing studies take advantage of Robert's equation to model the macroscopic behavior of molecules, that is, the concentration distribution, in space and time as:

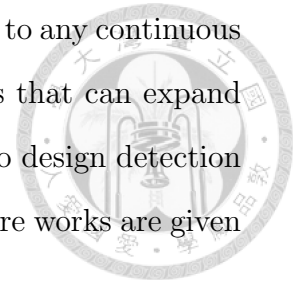
$$U(d, t) = N(4\pi Dt)^{-\frac{3}{2}} \exp\left(-\frac{d^2}{4Dt}\right), \quad (1.1)$$

where D is the diffusion coefficient. However, this form simply describes the *expectation* of the molecule behavior. The fluctuation or randomness of concentration level should be taken into account. This thesis is the first study that provides stochastic model for diffusion channel when continuous waveform is applied at TN. Based on the model, we also propose methods for solving a set of basis functions in order to achieve orthogonal expansion for detection.

1.4 *Thesis Organization*

The rest of the thesis is organized as follows. In Chapter 2, we provide a one-dimensional modulation and detection scheme, under which we design an ISI cancellation algorithm that dramatically improves the system performance. In Chapter 3, we consider a more complicated modulation which embeds information on both quantity and type of molecules. This modulation combats both ISI effect and background noise simultaneously. We also provide principles to choose system parameters to achieve good performance. In Chapter 4 of this thesis, we construct a stochastic model for the diffusion channel starting from Brownian motion of each

molecule. Different from the results in [10,12], this model applies to any continuous wave transmitted by TN. We also solve a set of basis functions that can expand the received signals into observation vectors, which enables us to design detection criterion for different modulations. Finally, conclusions and future works are given in Chapter 5.



CHAPTER 2

QUANTITY MODULATION



2.1 Introduction

In this chapter, we study the communication between two nano-machines with information embedded in different molecular quantity [13]. In the rest of this chapter, we call this kind of modulation as quantity modulation (QM). It is known that in diffusion-based molecular communications, molecules are emitted by the transmitter and move towards the receiver following the laws of molecule diffusion. Recent studies on diffusion-based molecular communications often model the statistical behavior of molecule diffusion as a Brownian motion [8]. Due to the random nature of Brownian motions, molecules that released earlier by TN may arrive late. Therefore, messages carried in current molecules may be interfered by those delayed molecules that were transmitted earlier. This phenomenon is known as the ISI effect in diffusion-based molecular communications. Studies about this effect can be found in [14] and [15].

There are lots of ways to design filters to eliminate the effect of ISI in conventional communication such as linear equalizer, adaptive equalizer and decision-feedback equalizer [16]. However, both linear equalizer and adaptive equalizer do not work well in molecular communication due to time-varying channel response. In this chapter, we utilize the concept of decision feedback and introduce a method to mitigate the effect of ISI.

The rest of this chapter is organized as follows: In Sec. 2.2, we introduce the settings of a binary QM molecular communication system in details. We also describe the characteristics and the mathematical model of a Brownian motion channel. Sec. 2.3 focuses on deriving the decision rule for one-shot transmission of the binary QM system and extending it to the M-ary transmission case. In

Sec. 2.4, we consider serial transmission and take ISI effect into account. ISI cancellation method is also described in this section. Numerical results are shown in Sec. 2.5.



2.2 System Model

In this section, we first give a general model for transmitter, receiver, and channel in molecular communication. We then describe a QM system of M quantity levels (M -ary modulation) bearing $\log_2 M$ information bits, which will be used later to apply our ISI cancellation method.

2.2.1 Transmission Nano-machine

Fig. 3 illustrates a transmitter nano-machine TN transmitting molecules to a receiver nano-machine RN. When TN obtains information (e.g. bit pattern) to be transmitted, it starts storing certain number of molecules in a vesicle (container that stores molecules) and releases these molecules simultaneously into the environment. The number of released molecules differs according to the transmitting information. In practical situations, molecules leaves the vesicle with random timing which is discussed in [17]. In this thesis, we simply assume that molecules exit the vesicle simultaneously.

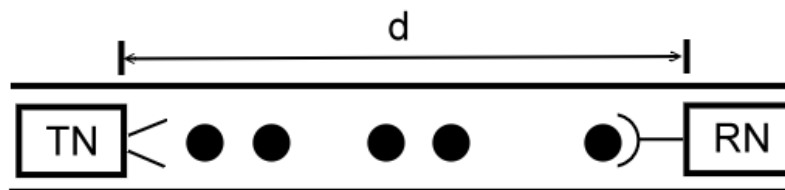


Figure 3: Transmission from TN to RN through a fluid medium.

2.2.2 Reception Nano-machine

RN is located at a position $d > 0$ apart from TN. There are several receptors capturing molecules on RN. RN counts the number of molecules it captures and perform detection according to the number. We assume the molecules can

be perfectly captured by the receptors and RN does not have counting errors. Furthermore, once a molecule arrives at RN, it will be removed from the communication medium.



2.2.3 Channel

Consider a fluid medium between TN and RN with positive drift velocity v . The molecules are all constrained to move in a one-dimensional space. We assume that the trajectory of emitted molecules can be modeled with independent Brownian motions [8]. Let X denote the random variable representing the first hitting time of a molecule. If $v > 0$, it can be shown that the probability density function (PDF) of X is given by the inverse Gaussian (IG) distribution [18]

$$f_X(x) = \begin{cases} \sqrt{\frac{\lambda}{2\pi x^3}} \exp\left\{-\frac{\lambda(x-\mu)^2}{2\mu^2 x}\right\}, & x > 0, \\ 0, & x \leq 0, \end{cases} \quad (2.1)$$

$$\mu = \frac{d}{v} \text{ and } \lambda = \frac{d^2}{2D},$$

where D denotes the diffusion coefficient which is given by

$$D = \frac{k_B T_a}{6\pi\tau r},$$

where k_B is the Boltzmann constant, T_a is the absolute temperature, τ is the viscosity of the fluid medium, and r is the radius of molecules. For simplicity, we assume that the radii for all molecules are the same so that the diffusion coefficients are the same.

2.2.4 QM System

Consider a time-slotted M -ary communication with signaling interval T_B , TN can release M different quantities of molecules into the channel. Denote those M quantities by L_m , where $m \in \{0, 1, 2, \dots, (M-1)\}$. Assume the *a priori* probability for releasing L_m molecules to be q_m . At the starting time of each transmission

time slot, L_m molecules are emitted simultaneously from the transmitter to indicate the transmission of a symbol. We assume perfect synchronization between the transmitter and the receiver. During each time slot, RN counts the total number of arriving molecules. An appropriate decision rule, proposed in Sec. 2.3, is then applied to determine the transmitted data bit at the end of each time slot. The molecules which fail to arrive within the corresponding time slot become a source of interference, which will cause performance degradation to the detections of later coming symbols. Fig. 4 is an example of QM system with $M = 4$ and uniform quantity levels.

Perfect synchronization between TN and RN is assumed in this chapter, a possible realization which is based on sending training molecular impulses are introduced in [BoKai].

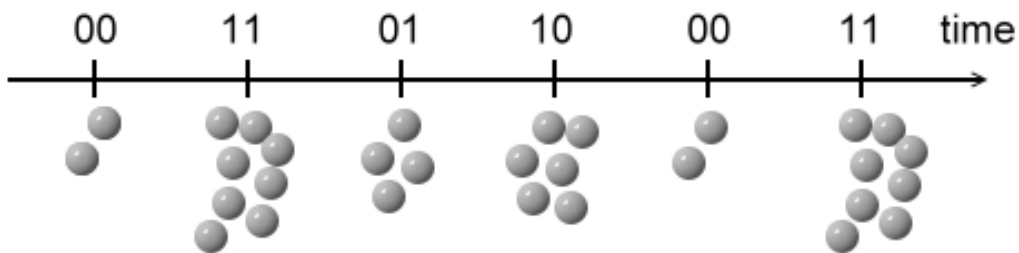


Figure 4: Illustration of quantity-based modulation scheme with $L_0 = 2$, $L_1 = 4$, $L_2 = 6$, $L_3 = 8$.

2.3 Detection in One-shot Transmission

In this section, we discuss the detection rule of the system for one-shot transmission. The main contribution of our work is that we separate the ISI cancellation problem from the detection to achieve a more flexible and modularized design, which is different from previous works [19].

2.3.1 Binary Detection

We define two hypotheses H_0 and H_1 . H_0 is the hypothesis that L_0 molecules are transmitted (indicating bit 0), and H_1 is the hypothesis that L_1 molecules are transmitted (indicating bit 1). Denote the conditional PDF of the number of

received molecules in a particular time slot, given that hypothesis H_m is true, by $\Pr\{N = n|H_m\}$, $m \in \{0, 1\}$. Using the inverse Gaussian PDF given in (2.1), we define the probabilities p_j as:

$$p_j = \int_{jT_s}^{(j+1)T_s} f_X(x) dx \quad (2.2)$$

for $j \in \{0, 1, \dots\}$, which is the probability that the traveling time of a molecule falls in the interval $[jT_s, (j+1)T_s]$, where j is the index of the time slots. Define Y_k to be the indicator random variable showing whether the k -th molecule emitted in a one-shot transmission arrives within T_s given that H_m is true. That is,

$$Y_k = \begin{cases} 1, & \text{if the } k\text{-th molecule arrives within } T_s, \\ 0, & \text{otherwise.} \end{cases} \quad (2.3)$$

Let N be the random variable denoting the total number of molecules arriving at the receiver within a particular time slot. We have the following relation:

$$\Pr\{N = n|H_m\} = \Pr\{Y_1 + Y_2 + \dots + Y_{L_m} = n|H_m\}. \quad (2.4)$$

Given the number of the transmitted molecules, N thus follows Binomial(L_m, p_0). For large L_m , we approximate the binomial distribution by a Gaussian distribution with the knowledge of the mean and variance of N . Namely, we have

$$\Pr\{N = n|H_m\} \approx \frac{\exp\left\{-\frac{(n - L_m p_0)^2}{2L_m p_0(1 - p_0)}\right\}}{\sqrt{2\pi L_m p_0(1 - p_0)}}. \quad (2.5)$$

As a special case when $M = 2$, the distributions of N under two hypotheses can thus be obtained as

$$\Pr\{N = n|H_0\} \approx \frac{\exp\left\{-\frac{(n - L_0 p_0)^2}{2L_0 p_0(1 - p_0)}\right\}}{\sqrt{2\pi L_0 p_0(1 - p_0)}}, \quad (2.6)$$

$$\Pr\{N = n|H_1\} \approx \frac{\exp\left\{-\frac{(n - L_1 p_0)^2}{2L_1 p_0(1 - p_0)}\right\}}{\sqrt{2\pi L_1 p_0(1 - p_0)}}. \quad (2.7)$$

According to the conventional hypothesis testing theory [20, 21], the decision rule can be expressed using the likelihood ratio test $\Lambda(N)$ as

$$\Lambda(N) = \frac{P(N|H_1)}{P(N|H_0)} \underset{H_0}{\overset{H_1}{\gtrless}} \frac{q_0}{q_1}. \quad (2.8)$$

If we assume equal *a priori* probabilities $q_0 = q_1 = 1/2$, due to the characteristic of Gaussian distribution shown in Fig. 5, the decision rule can be further reduced to

$$N \underset{H_0}{\overset{H_1}{\gtrless}} \eta \quad (2.9)$$

for some threshold η , where η is the solution of the following equation:

$$\Pr\{N = \eta|H_0\} = \Pr\{N = \eta|H_1\}. \quad (2.10)$$

By (2.6) and (2.7), we have

$$\sqrt{\frac{L_1}{L_0}} = \exp \left\{ \frac{(L_1 - L_0)(\eta^2 - p_0^2 L_0 L_1)}{2L_0 L_1 p_0 (1 - p_0)} \right\}. \quad (2.11)$$

Taking logarithms to both sides, the equation becomes

$$\eta = \sqrt{\frac{L_1 L_0 \ln(L_1/L_0)}{L_1 - L_0} p_0 (1 - p_0) + p_0^2 L_0 L_1}. \quad (2.12)$$

In other words, if the received number of molecules is greater than the threshold η , the receiver will determine H_1 as the hypothesis testing result; otherwise H_0 will be decided.

2.3.2 M-ary Detection

The detection rule can be extended to M -ary detection with only a few adjustments. Suppose we have multiple hypotheses H_m where $m \in \{0, 1, 2, \dots, (M-1)\}$ which represent the transmission of L_m molecules. The goal is to decide which \hat{m} we should choose. The maximum *a priori* (MAP) detection rule is:

$$\hat{m}(N) = \underset{m}{\operatorname{argmax}} P(N|H_m). \quad (2.13)$$

Due to the properties of Gaussian distribution, the above MAP detection rule can be simplified to pairwise comparisons between the “neighboring” conditional probability distributions.

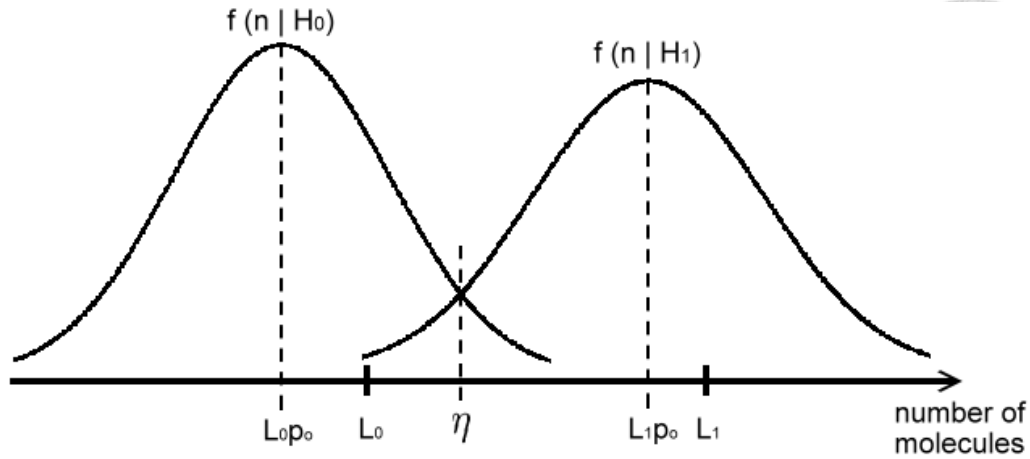


Figure 5: Demonstration of the process of finding η in a binary QM system, where f is the conditional PDF of N given H_m is true.

To write down the expressions explicitly, we define a set of thresholds $E = \{\eta_j \in [-\infty, \infty] : j = 0, 1, 2, \dots, M\}$, and let $\eta_0 = -\infty$ and $\eta_M = \infty$. For $j = 1, 2, \dots, (M - 1)$, η_j can be obtained by solving the equations

$$\Pr\{N = \eta_j | H_{j-1}\} = \Pr\{N = \eta_j | H_j\}. \quad (2.14)$$

With the thresholds determined, the detection rule for M -ary transmission can be expressed as

$$\hat{m}(N) = \sum_{k=0}^{M-1} k \cdot u[-(N - \eta_k)(N - \eta_{k+1})]. \quad (2.15)$$

where $u(\cdot)$ denotes the unit step function.

2.3.3 Error Rate Analysis

After the construction of the transmission and decision rules, we then analyze how it performs in terms of symbol or bit error rate. Consider a specific case for $M = 2$ and $q_0 = q_1 = 1/2$. Denote the false alarm probability as P_F and the missing probability as P_M . The error rate can be written as

$$P_e = q_0 P_F + q_1 P_M = \frac{1}{2}(P_F + P_M). \quad (2.16)$$

From Fig. 5 and the decision rule derived in Sec. 2.3.1, it can be shown that

$$P_F = \Pr\{N > \eta | H_0\} = Q\left(\frac{\eta - L_0 p_0}{\sqrt{L_0 p_0 (1 - p_0)}}\right), \quad (2.17)$$

$$P_M = \Pr\{N < \eta | H_1\} = Q\left(\frac{L_1 p_0 - \eta}{\sqrt{L_1 p_0 (1 - p_0)}}\right), \quad (2.18)$$

where $Q(\cdot)$ denotes the Q-function. By substituting (2.12) into equation (2.17) and (2.18), we can evaluate the error rate P_e in (2.16). Fig. 6 shows the comparison between our analysis and numerical results.

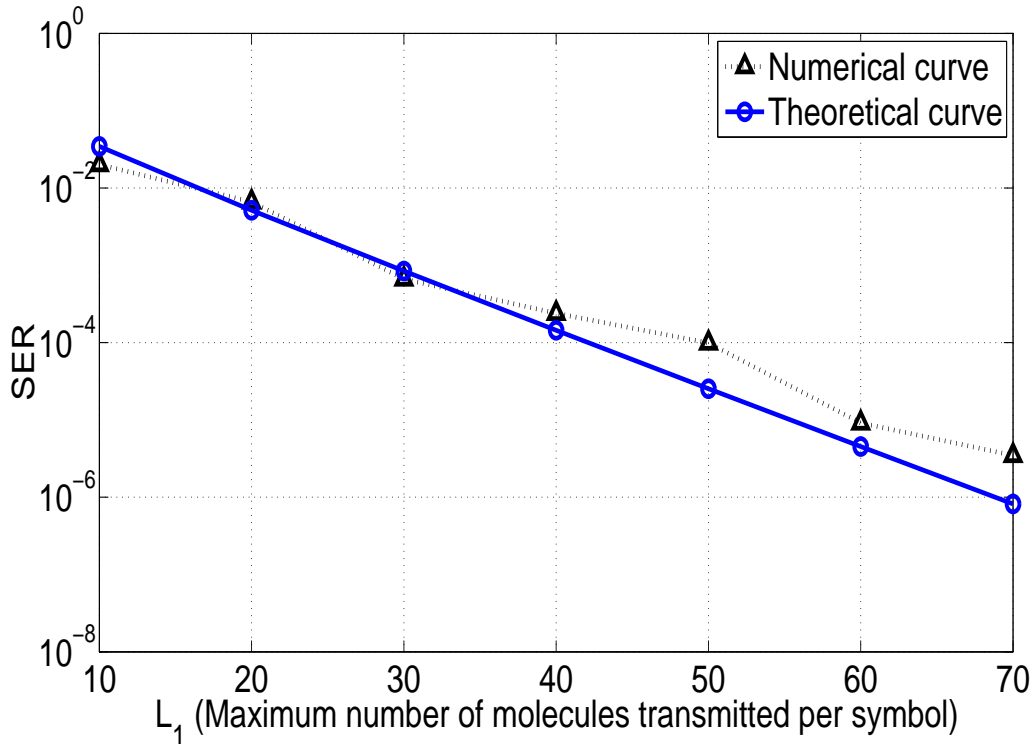


Figure 6: Theoretical result versus numerical result for one-shot binary quantity-based modulation.

2.4 Serial Transmission and ISI Cancellation

The above described QM molecular communication system seems to work already. However, in practical situations, we need to perform serial transmissions rather than one-shot transmission. Thus the ISI effect must be taken into account. Our results show that if we do not modify our one-shot detection rule, the system performance will fall dramatically under serial transmission environments due to the severe ISI effect. To solve this problem, we propose a method to mitigate the ISI effect.

In order to mitigate the ISI effect, we first need an estimation of the number of

the delayed molecules that come from former time slots. If we know the conditional probability distribution of the number of ISI molecules conditioned on the current received number, then we can estimate the ISI effect as the conditional mean. However, the conditional distribution does not have a closed-form solution for inverse Gaussian random variables. Here, we proposed another intuitive way to do this estimation.

First, we define “memory- Γ cancellation” to mean that the ISI effect during the past Γ time slots are taken into account when making decision. We first use memory-1 cancellation as a demonstrative example. If the number of molecules received during the $(i-1)$ -th time slot is n_{i-1} and the decided transmission quantity level is \hat{l}_{i-1} , where $\hat{l}_{i-1} \in \{L_0, L_1, \dots, L_{M-1}\}$, we then subtract $\hat{l}_{i-1} \cdot [F_X(2T_s) - F_X(T_s)]$ (the *a priori* expected received number in the i -th time slot from the $(i-1)$ -th time slot) from n_i before making the i -th decision, where $F_X(\cdot)$ is the cumulative distribution function (CDF) of the first-hitting time of molecules. In other words, the actual number \tilde{n}_i used in making decision is

$$\tilde{n}_i = n_i - \hat{l}_{i-1} \cdot [F_X(2T_s) - F_X(T_s)]. \quad (2.19)$$

Likewise, we can perform memory- Γ cancellation if we have enough buffer at the receiver end to memorize temporarily the recently received numbers of molecules. More explicitly, denote the probabilities that a single transmitted molecule arrives during the time interval $[jT_s, (j+1)T_s]$ by p_j for $j \in \mathbb{N} \cup \{0\}$ as before. If the decided transmission quantity level of the current time slot is \hat{l} , where $\hat{l} \in \{L_0, L_1, \dots, L_{M-1}\}$, then the received number of molecules j time slots later should be subtracted by $\hat{l} \cdot p_{j+1}$ before making decision. In other words, if the number of molecules received in i -th time slot is n_i , the actual number \tilde{n}_i used in making decision is

$$\tilde{n}_i = n_i - \sum_{j=1}^{\Gamma} \hat{l}_{i-j} p_{j+1}. \quad (2.20)$$

For binary QM systems, the decision rule can be written as

$$\tilde{n}_i = n_i - \sum_{j=1}^{\Gamma} \hat{l}_{i-j} p_{j+1} \underset{H_0}{\overset{H_1}{\geq}} \eta. \quad (2.21)$$

The extension to M-ary QM systems is straightforward.

2.5 Numerical Results

In this section, we first discuss the binary and M -ary QM modulation systems with and without performing ISI cancellation. After that, we make comparisons of the system performance under different time slot durations.

The number of molecules is one of the main resources utilized in molecular communications. Analogous to the “power” concept in conventional communications, we need to take this number into account when comparing the system performances. In the following subsections, we present the results under different maximum number of molecules allowed per symbol, and the quantity levels are uniformly spaced. The simulation parameters are $d = 0.2$ cm, drift velocity $v = 0.01$ cm/sec, diffusion coefficient $D = 0.05$ cm²/sec, and time slot duration $T_s = 5$ sec.

2.5.1 SER Comparison with and without ISI Cancellation

In Fig. 7, a binary transmission system with memory-1 and memory-2 cancellation is considered. The SER drops from 0.04 to 0.01 when $L_1 = 30$, and drops from 10^{-2} to 10^{-4} when $L_1 = 90$. The improvement grows as L_1 increases, which means that by choosing L_1 properly, a reliable end-to-end transmission can be achieved. We also observe that even without ISI cancellation, the error rate will drop as L_1 increases. The reason is that the spacing between symbols is increased. However, as shown in Fig. 8, it is not the case for the quaternary transmission system. It can be seen that even though L_3 becomes large, the error rate is still high without ISI cancellation, which means we cannot rely solely on increasing the maximum number of molecules without ISI cancellation.

It is worth mentioning that the ISI cancellation method can be performed not only in such quantity-based modulation systems, but it can also be used in other systems like on-off keying¹ with slight modifications.

¹Transmitting zero or a single molecule.



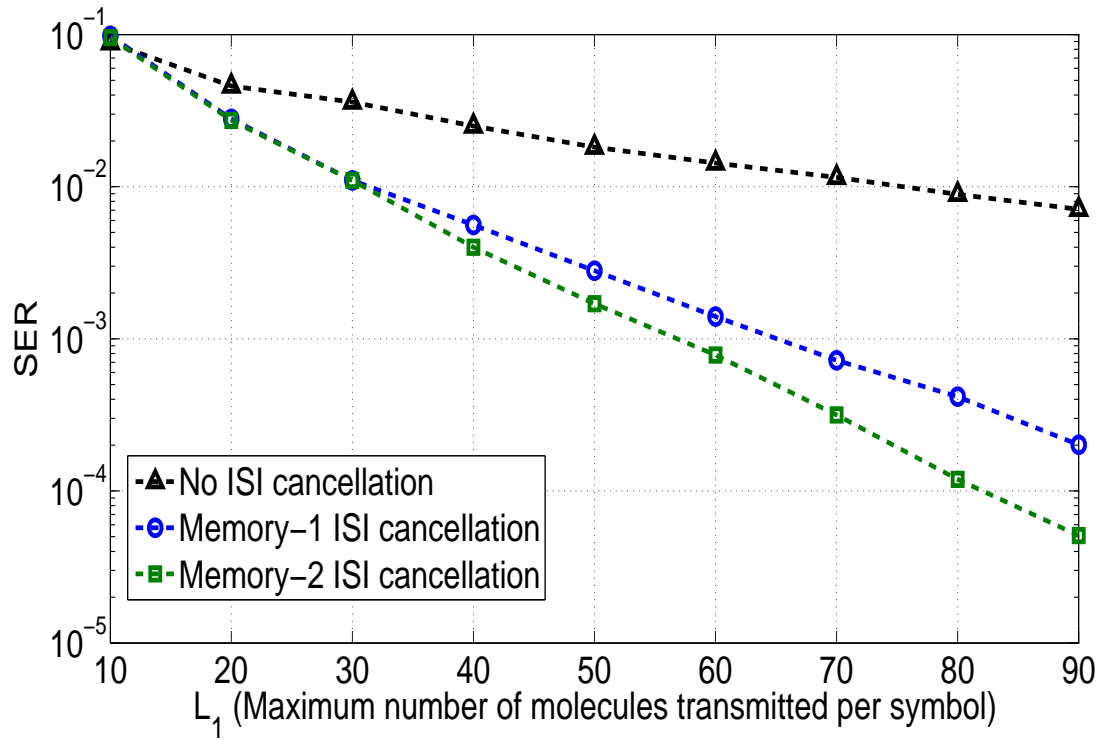


Figure 7: Binary quantity-based modulation with ISI cancellation.

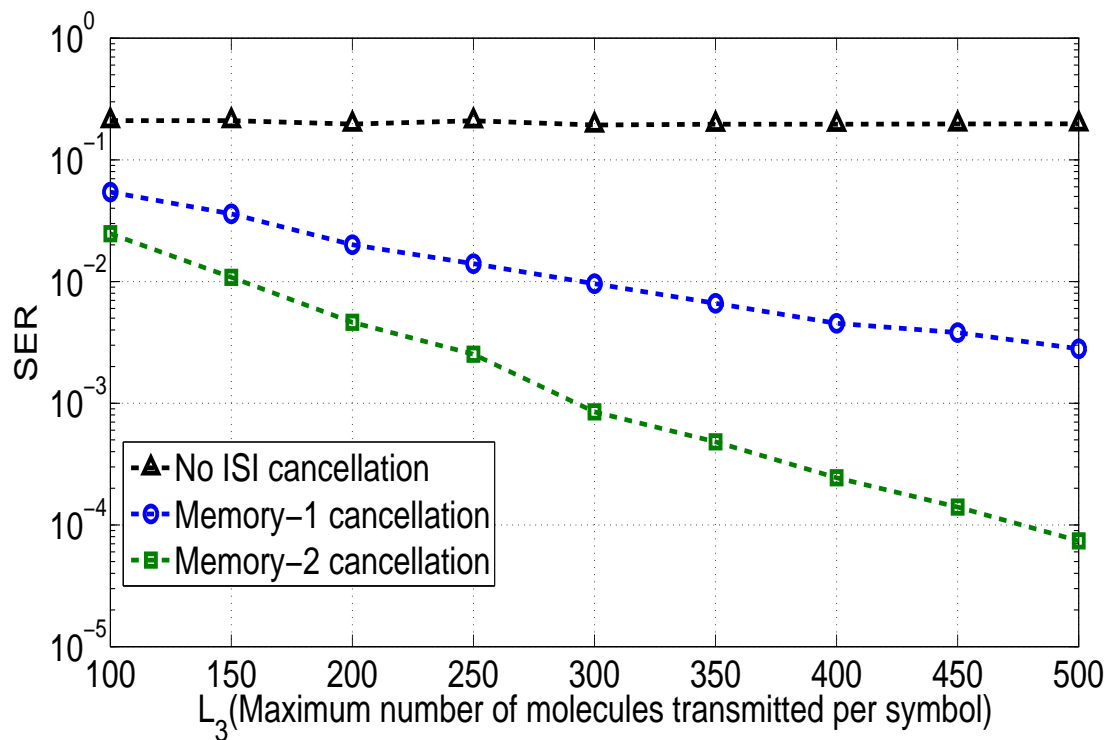


Figure 8: Quaternary quantity-based modulation with ISI cancellation.

2.5.2 Performance Under Different Duration of Time Slot

In this subsection, we consider a binary transmission system with and without ISI cancellation for different time slot durations. From Fig. 9, we can observe that the SER decreases as the duration T_s increases. In other words, to improve performance, one can increase the duration of the time slot as shown in Fig. 9. Although the error rate is already quite acceptable, it can be further improved by the ISI cancellation approach. The improvements is about 10 times better when $T_s = 10$ sec and $L_1 = 70$. Note that when T_s is small, say $T_s = 1$ sec, compared to the expected first-hitting time d/v , the error rate increases even if we increase L_1 when no cancellation is performed. This is because when T_s is small, molecules tend not to arrive in one symbol time but stay in the background, and that a larger L_1 will cause a larger amount of molecules to be in the background and hence larger interference.

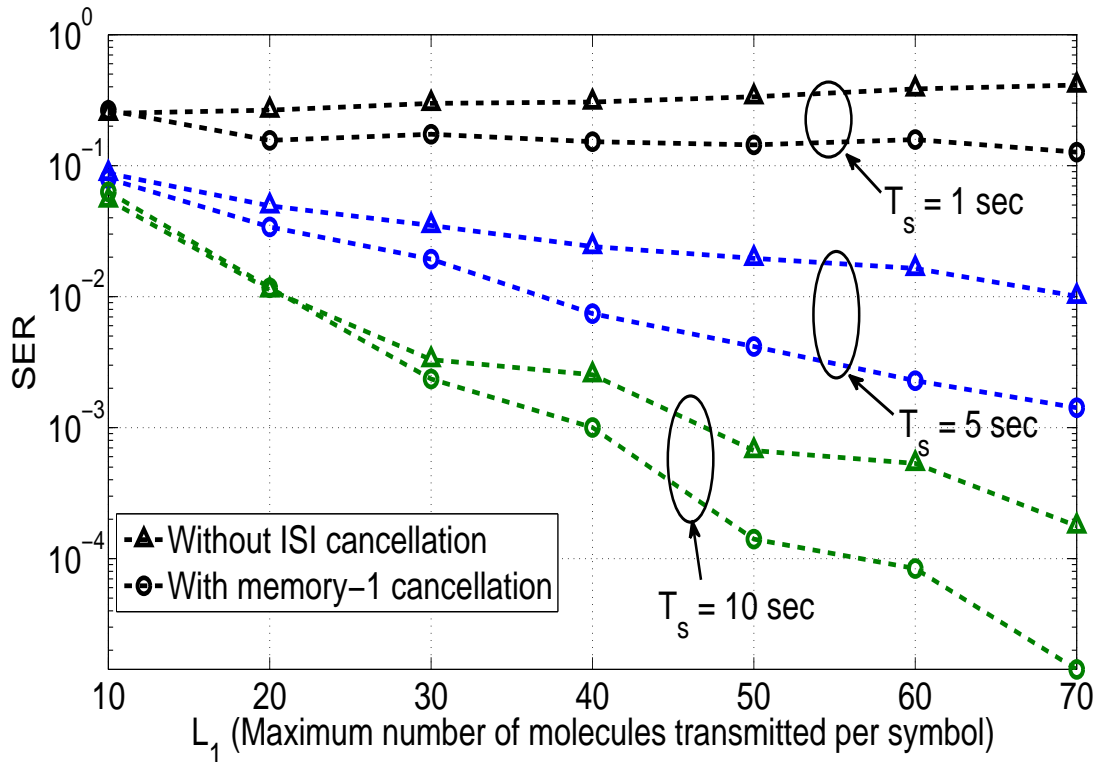


Figure 9: Binary quantity-based modulation with ISI cancellation under different T_s .

CHAPTER 3

QUANTITY-TYPE MODULATION

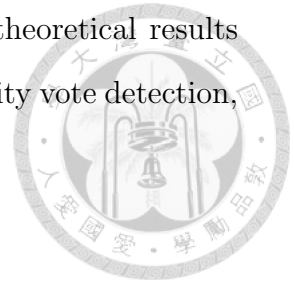


3.1 Introduction

To communicate between two nano-machines, several modulation techniques have been proposed to bear information [10, 12, 22–25]. Among various kinds of modulation, quantity [22] and type [23, 24] modulation is of our interests. Based on the design paradigms of both works, that the type of molecules could yield additional embedded information, and that the increase in the quantity of molecules per transmission could result in higher performance, we propose a new modulation scheme called *quantity-type* modulation. Consider a type-based modulated system, the transmitter releases different types of molecules representing different information bits or symbols. When the molecules arrive at the receiver, the receiver captures those molecules and attains information based on their types. Nevertheless, the arrival times of the molecules at the receiver are random due to the diffusion process. This results in the phenomenon that the molecules released earlier may arrive late, leading to wrong information detection. A way to remedy this is to release a group of molecules of the same type at a time to improve the system reliability.

An intuitive method to detect the quantity-type modulated molecular communication system is using majority vote—information bits are detected according to the type of molecules that outnumber another. However, as it is shown in this paper, the performance of the majority vote detection algorithm is disappointing. Hence, in this chapter, we introduce a novel detection algorithm called *threshold-based detection* by exploiting the characteristics of the diffusion channel. Theoretical approximations of the bit error rate (BER) performance of the proposed threshold-based detection algorithm for the quantity-type-modulated molecular

communication system are derived. Both the simulation and theoretical results confirm the significant performance improvement over the majority vote detection, either without or with background noise.



3.2 System Model

In this section, based on the diffusion channel modeled by Brownian motion as in 2.2, we introduce the communication scheme adopted in this chapter.

3.2.1 Quantity-type Modulation

We assume that two types of information molecules, ‘A’ and ‘B’, have the same radius r and are distinguishable for both transmitter and receiver. This can be achieved by using isomers as described in [26]. The transmission is assumed to be time-slotted with interval T_s and the transmitter releases n molecules of one type at the beginning of each time slot to represent an information bit, where n is an odd number. That is, n type-A molecules represent bit ‘1’ and n type-B molecules represent bit ‘0’. In addition, the information bits are firstly partitioned into blocks with L bits. When nL molecules are released, the transmitter should wait for a period of time T before the next transmission. The receiver always gathers molecules on arrival, that is, there is no fixed time slots at the receiver and the asynchronous detection, i.e., majority-vote detection or threshold-based detection, is performed. Moreover, whenever nL molecules are captured, the receiver should also wait for a period of time T before the next detection. The waiting time between blocks is set to avoid detection errors caused by background noise (which will be mentioned in the next subsection) affecting the next block.

3.2.2 ISI and Noise Effect on Quantity-type Modulation

Due to the randomness of the first hitting times of transmitted molecules, a molecule may arrive at the receiver in advance of the molecule(s) released earlier. We use the term *crossover* to describe this phenomenon. Crossovers result in intersymbol interference (ISI) and may lead to detection errors.

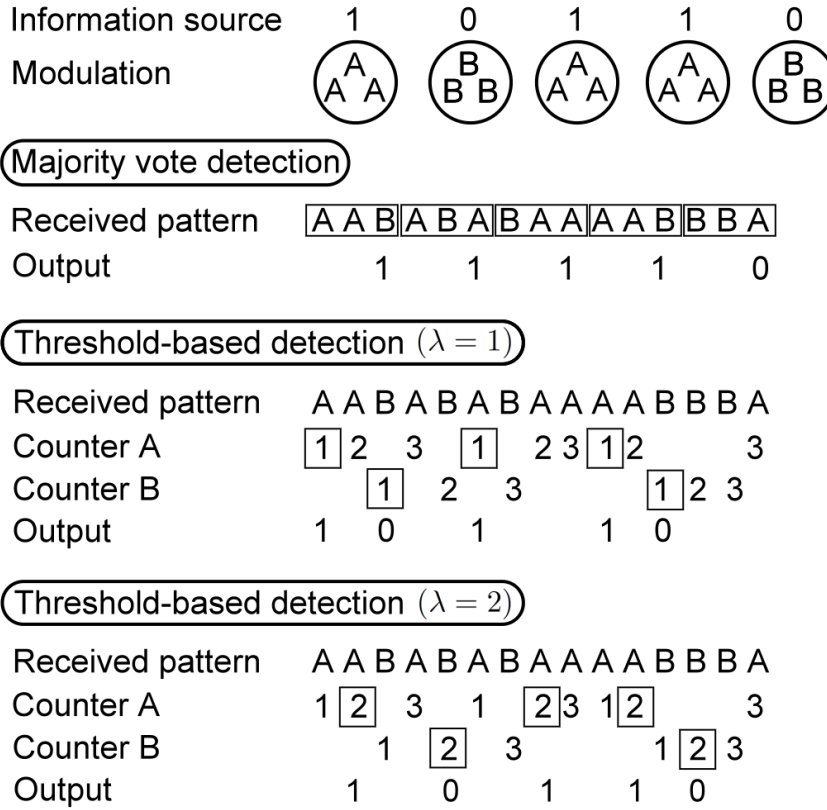


Figure 10: A demonstrative example for the majority-vote detection algorithm and the threshold-based detection algorithm with $\lambda = 1$ and $\lambda = 2$. The boxed numbers represent the value stored in the counter that reaches the threshold λ .

In diffusion-based molecular communications, it is likely for the receiver to capture molecules that are not released by the corresponding transmitter. Those unintended molecules, which we call *background noise* in the rest of this study, may come from the environment or other transmitters. We model the number of arriving unintended molecules as a Poisson random process $\{N(t) : t \geq 0\}$ and $N(t + \tau) - N(t)$ follows $\text{Poisson}(\alpha\tau)$ with noise rate α .

3.3 Detection Algorithms

In this section, we first describe the majority-vote detection algorithm and then elaborate the proposed threshold-based detection algorithm.

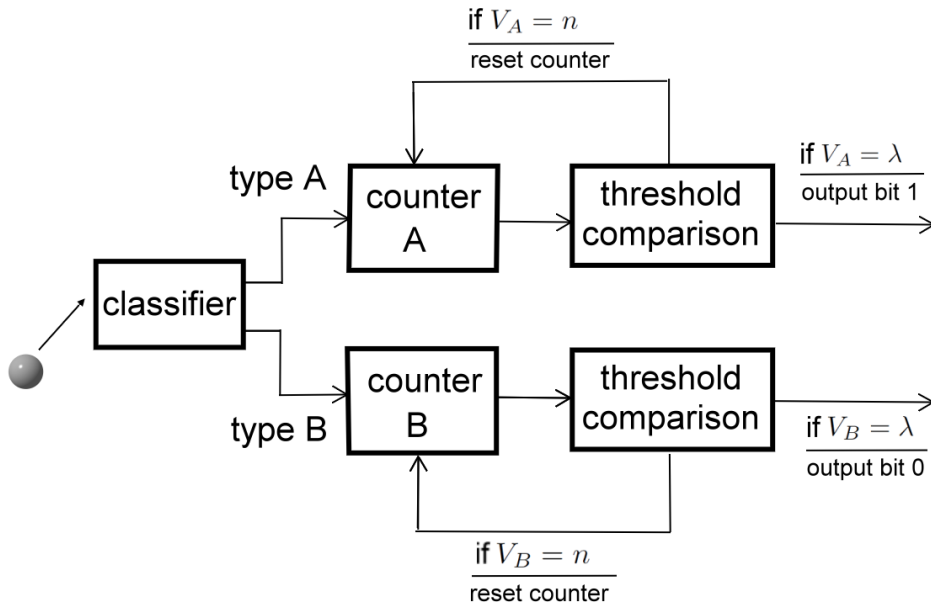


Figure 11: Block diagram of the threshold-based detection algorithm.

3.3.1 Majority-vote Detection

An intuitive detection method of the quantity-type-modulated molecular communication system is the majority vote, which counts the majority type of molecules once n molecules are gathered. We use an example to explain the majority-vote detection in Fig. 10. To illustrate that different types of molecules are released by the transmitter at different time slots, we use $(\mathbf{U}_1, \mathbf{U}_2, \mathbf{U}_3, \dots)$ to represent that the transmitter releases a set of molecules \mathbf{U}_1 at $t = t_0$, molecules \mathbf{U}_2 at $t = t_0 + T_s$, and molecules \mathbf{U}_3 at $t = t_0 + 2T_s$, and so on. Let us consider the example in Fig. 10, the transmitter releases (AAA, BBB, AAA, AAA, BBB) to convey the information sequence ‘1, 0, 1, 1, 0’. Due to the diffusion channel, the arriving molecules may be out of order. In this example, the receiver captures the molecules in the order of

$$\text{‘A, A, B, A, B, A, B, A, A, A, A, B, B, B, A’}. \quad (3.1)$$

Note that in both (3.1) and “Received pattern” in Fig. 10, we do not show the time difference between two adjacently captured molecules, which may not be identical. The majority-vote algorithm groups the molecules as ‘A, A, B’, ‘A, B, A’, ‘B, A,

A', 'A, A, B', and 'B, B, A', and determines the majority type in each group as 'A', 'A', 'A', 'A', and 'B'. Therefore, the detected bits are '1, 1, 1, 1, 0', which has one bit error. This error results from the effect of ISI as described in Sec. 3.2.2.

3.3.2 Threshold-based Detection

To develop a detection algorithm that is suitable for operating under the diffusion channel, let us first gain some insights about how the diffusion-based molecular communication system is performed. Consider a case that the transmitter releases (A, B), i.e., the transmitter releases a molecule of type A and then a molecule of type B after a time duration T_s . It is likely that the receiver receives 'B, A', which results in bit errors. However, if the transmitter releases (AAA, BBB), i.e., the transmitter releases three molecules of type A and then three molecules of type B after a time duration T_s , the probability that the receiver receives 'B, B, B, A, A, A' is small since it requires many crossovers happening to obtain this pattern. It is more likely that at least one type-A molecule arrives earlier than all the type-B molecules. Therefore, a reasonable principle for designing detection algorithm would be: once the receiver captures a type-A molecule before capturing a type-B molecule, the receiver infers that the transmitter releases (AAA) before (BBB). The remaining two type-A molecules that arrive later provide relatively little information, and they may even introduce ISI to other molecules; hence the receiver should ignore those two late-arriving molecules.

Based on the above observation, we propose the threshold-based detection algorithm. As shown in Fig. 11, the detector is composed of a classifier, two counters, and two threshold comparators. The classifier recognizes the type of the arriving molecules. If the arriving molecule belongs to type A, the classifier generates a signal to counter A; if the arriving molecule belongs to type B, the classifier generates a signal to counter B. Counter A and counter B are used to count the number of arriving molecules of type A and B, respectively. Whenever a signal is sensed by the counter, it increases its stored value by one. The values stored in the counters are denoted by V_A and V_B respectively. When the value stored in

the counter reaches a predetermined threshold λ , bit ‘1’ or ‘0’ is generated. Once the stored value reaches n , the stored value is reset to zero. Note that when V_A or V_B is in the region $(\lambda, n]$, no output is generated by the detector. That is, $n - \lambda$ molecules with the same type are ignored by the receiver.

Fig. 10 shows a simple example that does not consider the noise effect (or the noise rate α is negligibly small). The detection result in this example has no bit error. An example of the threshold-based detection algorithm considering the background noise is shown in Fig. 12. The transmitter releases three molecules at a time and the receiver applies the threshold-based detection with threshold $\lambda = 3$. In this example, only the background noise caused by type-A molecules is considered. The unintended molecules are equivalently inserted into the receiving molecule pattern. The inserted molecules cause wrong increment of the value stored in the counter, making the receiver output an erroneously detected bit. This is termed *bit insertion*. When this happens, the detected bit sequence is right-shifted compared with the actual bit sequence.

Since n molecules are released in each symbol duration, the total number of arriving molecules at the receiver should be nL for each block. However, due to the background noise, the total number of molecules may be greater than nL . The proposed scheme in Sec. 3.2.1 suggests that after nL molecules are received, the receiver ignores the late-arriving molecules for a period of T . We set $T = 2T_s$ since the probability that a molecule arrives late for more than $2T_s$ is small.

3.3.3 Trade-offs when Combating ISI and Noise Effect on Quantity-type Modulation

ISI comes from the crossover effect of the released molecules. Intuitively, adopting a larger signaling interval T_s at the transmitter will decrease the probability of crossovers. However, as T_s grows larger, the number of unintended molecules captured by the receiver during each symbol detection will increase. Thus, we expect that there should be an optimal T_s which minimizes the detection error caused by both ISI and background noise. The optimal T_s for threshold-based

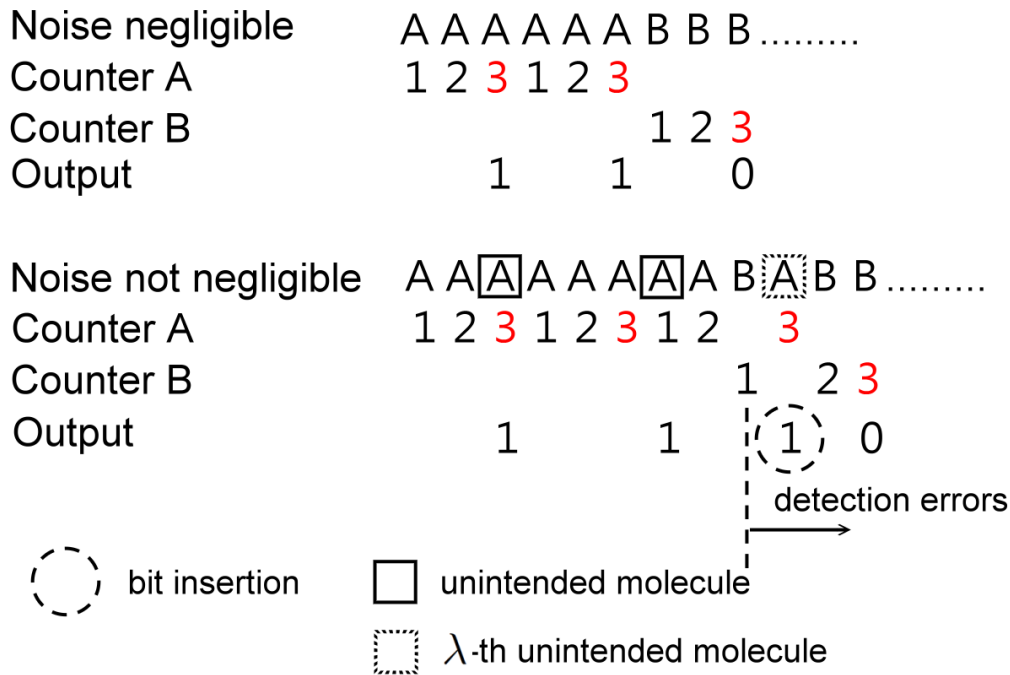


Figure 12: A demonstrative example for the detection result under background noise using the threshold-based detection algorithm. $\lambda = 3$. In the example, the crossover effect is not taken into account.

detection will be derived in Sec. 3.4.

It can be observed that detection errors occur when unintended molecules are captured by the receiver, which causes the value stored in the counter to reach the threshold λ too early. Therefore, to combat the background noise, we may increase the value of λ . However, as will be shown later, a small λ is better for combating ISI. Details in determining λ is discussed in Sec. 3.5. Moreover, the value of n also affects the system performance since $\lambda \leq n$, that is, n limits the possible choices of λ .

To deal with the background noise, it is also possible to modify the block size L . The effects of background noise can be mitigated by using a smaller L since the number of unintended molecules in a block can be reduced. Nevertheless, when a smaller block size is used, the total throughput decreases due to the longer duration between blocks.

In the next section, we analyze the system performance in the sense of bit

error rate (BER). Based on the BER performance, principles of choosing the above-mentioned system parameters will be discussed in Sec. 3.5.



3.4 BER Analysis

In this section, we mathematically compare the BER performance of the majority-vote detection algorithm and the proposed threshold-based detection algorithm. In the following, we first derive BER under the case that the background noise is negligible, i.e. α approaches zero. We then analyze the case when α is not negligible such that increasing T_s would introduce more unintended molecules at the receiver.

3.4.1 Preliminaries

For the i -th information bit $s_i \in \{0, 1\}$, n molecules of type A or B are released. By assuming that the prior probabilities $\Pr\{s_i = 0\} = \Pr\{s_i = 1\} = 1/2$, the BER can be written as

$$\begin{aligned} \Pr\{\hat{s}_i \neq s_i\} &= \frac{1}{2} \Pr\{\hat{s}_i = 1 | s_i = 0\} + \frac{1}{2} \Pr\{\hat{s}_i = 0 | s_i = 1\} \\ &= \Pr\{\hat{s}_i = 0 | s_i = 1\}, \end{aligned} \quad (3.2)$$

where \hat{s}_i is the information bit detected by the receiver. Equivalently, we can compute (3.2) by

$$\begin{aligned} \Pr\{\hat{s}_i \neq s_i\} &= \frac{1}{4} \Pr\{\hat{s}_i = 0 | s_{i-1} = 0, s_i = 1, s_{i+1} = 0\} + \frac{1}{4} \Pr\{\hat{s}_i = 0 | s_{i-1} = 0, s_i = 1, s_{i+1} = 1\} \\ &\quad + \frac{1}{4} \Pr\{\hat{s}_i = 0 | s_{i-1} = 1, s_i = 1, s_{i+1} = 0\} + \frac{1}{4} \Pr\{\hat{s}_i = 0 | s_{i-1} = 1, s_i = 1, s_{i+1} = 1\}. \end{aligned} \quad (3.3)$$

Each term in (3.3) is affected by the ISI from $\{s_{i-2}, s_{i-3}, \dots\}$ and $\{s_{i+2}, s_{i+3}, \dots\}$. Here, we assume that the errors due to crossover of molecules happening to neighboring information bits are dominant compared with the error due to crossover of molecules happening to information bits that are more than two time intervals apart. Therefore, we compute (3.3) by considering the relations of s_{i-1} , s_i , and s_{i+1} only.

Denote the first hitting time of the n molecules released for representing s_i as independent and identically distributed (i.i.d.) random samples $X_1(i), \dots, X_n(i)$. From the theorem of order statistics, if $X_1(i), \dots, X_n(i)$ are arranged in increasing order as $X_{(1)}(i) \leq \dots \leq X_{(n)}(i)$, the PDF and the cumulative density function (CDF) for the k -th smallest one are, respectively,

$$f_{X_{(k)}}(y) = n \binom{n-1}{k-1} F_X(y)^{k-1} [1 - F_X(y)]^{n-k} f_X(y), \quad (3.4)$$

and

$$F_{X_{(k)}}(y) = \sum_{j=k}^n \binom{n}{j} F_X(y)^j [1 - F_X(y)]^{n-j}, \quad (3.5)$$

where $F_X(y)$ is the CDF of X . Note that both (3.4) and (3.5) are defined on $y > 0$.

Now we define the *switching* between two symbols s_i and s_j as the event $\hat{s}_i = s_j, \hat{s}_j = s_i$ for $s_i \neq s_j$. For convenience, we define the events E_{pqr} and \hat{E}_{pqr} respectively as

$$\begin{aligned} E_{pqr} &= \{s_{i-1} = p, s_i = q, s_{i+1} = r\}, \\ \hat{E}_{pqr} &= \{\hat{s}_{i-1} = p, \hat{s}_i = q, \hat{s}_{i+1} = r\}. \end{aligned} \quad (3.6)$$

We use the superscript to distinguish the majority-vote detection and the threshold-based detection for \hat{s}_i and \hat{E}_{pqr} , i.e., \hat{s}_i^{MVD} and $\hat{E}_{pqr}^{\text{MVD}}$ for the majority-vote detection, and \hat{s}_i^{TD} and $\hat{E}_{pqr}^{\text{TD}}(\lambda)$ for the threshold-based detection with threshold λ .

3.4.2 Analysis when Background Noise is Negligible

Let us begin by analyzing the majority-vote detection. To calculate the BER of the majority-vote detection, denoted by P_c^{MVD} , (3.3) is rewritten as

$$\begin{aligned} P_c^{\text{MVD}} &= \Pr\{\hat{s}_i^{\text{MVD}} \neq s_i\} \\ &= \frac{1}{4} \Pr\{\hat{s}_i^{\text{MVD}} = 0 | E_{010}\} + \frac{1}{4} \Pr\{\hat{s}_i^{\text{MVD}} = 0 | E_{011}\} + \frac{1}{4} \Pr\{\hat{s}_i^{\text{MVD}} = 0 | E_{110}\} \\ &\quad + \frac{1}{4} \Pr\{\hat{s}_i^{\text{MVD}} = 0 | E_{111}\}. \end{aligned} \quad (3.7)$$

In the first term of (3.7), given E_{010} , the event $\hat{s}_i = 0$ happens when either of the following conditions is satisfied:

1. Molecules representing s_i cross over molecules representing s_{i+1} and then the event $\widehat{E}_{001}^{\text{MVD}}$ happens.
2. Molecules representing s_{i-1} cross over molecules representing s_i and then the event $\widehat{E}_{100}^{\text{MVD}}$ happens.
3. Molecules representing s_{i-1} , s_i , and s_{i+1} cross over in the way that the type-B molecules outnumber type-A molecules for all three detected symbols, and then the event $\widehat{E}_{000}^{\text{MVD}}$ happens.



Note that the above observation is made with the assumption in Sec. 3.4.1 that detection errors due to ISI is dominated by the crossovers of molecules from neighboring information bits, namely, s_{i-1} and s_{i+1} . Fig. 13 shows example outcomes given the event E_{010} which corresponds to the conditions mentioned above: the first outcome results from two crossovers between s_i and s_{i+1} , the second outcome results from two crossovers between s_i and s_{i-1} , and the third outcome results from one crossover between s_i and s_{i+1} and one between s_i and s_{i-1} . The second and third terms in (3.7) follow similar arguments. Given E_{011} or E_{110} , the event $\widehat{s}_i = 0$ is equivalent to $\widehat{E}_{101}^{\text{MVD}}$. The final term in (3.7) equals 0 since given event E_{111} , $\widehat{s}_i = 0$ is impossible. Therefore, by the assumption in Sec. 3.4.1, we have

$$P_c^{\text{MVD}} \approx \frac{1}{4} \Pr\{\widehat{E}_{001}^{\text{MVD}} \cup \widehat{E}_{100}^{\text{MVD}} \cup \widehat{E}_{000}^{\text{MVD}} | E_{010}\} + \frac{1}{4} \Pr\{\widehat{E}_{101}^{\text{MVD}} | E_{011}\} + \frac{1}{4} \Pr\{\widehat{E}_{101}^{\text{MVD}} | E_{110}\}. \quad (3.8)$$

To further compute (3.8), we need the following lemma.

Lemma. *Assume that the switching other than s_i and s_{i+1} is negligible. Under the quantity-type modulation and majority-vote detection without background noise, two transmitted symbols s_i and s_{i+1} switch if and only if $s_i \neq s_{i+1}$, and the order statistics $X_{(\frac{n+1}{2})}(i)$ and $X_{(\frac{n+1}{2})}(i+1)$ satisfy*

$$X_{(\frac{n+1}{2})}(i) > X_{(\frac{n+1}{2})}(i+1) + T_s. \quad (3.9)$$

Proof. Without loss of generality, we assume that $s_i = 1$ and $s_{i+1} = 0$. For the “if” part, the condition (3.9) is equivalent to having the crossover between the

$\frac{n+1}{2}$ -th molecule in s_i and the $\frac{n+1}{2}$ -th molecule in s_{i+1} . Therefore, (3.9) guarantees that there are at most $\frac{n-1}{2}$ molecules of type A arriving earlier than $X_{(\frac{n+1}{2})}(i)$, and there are at least $\frac{n+1}{2}$ molecules of type B arriving earlier than $X_{(\frac{n+1}{2})}(i)$. Since $\frac{n-1}{2} + \frac{n+1}{2} = n$, we conclude that for the majority-vote detection, the detection results are $\hat{s}_i = 0$ and $\hat{s}_{i+1} = 1$, i.e., s_i and s_{i+1} switch.

For the “only if” part, we assume that either $s_i = s_{i+1}$ or $X_{(\frac{n+1}{2})}(i) < X_{(\frac{n+1}{2})}(i+1) + T_s$, and we aim to prove s_i and s_{i+1} do not switch. The first case $s_i = s_{i+1}$ is trivial since no switching happens between two identical symbols. For the other case $X_{(\frac{n+1}{2})}(i) < X_{(\frac{n+1}{2})}(i+1) + T_s$, there are exactly $\frac{n+1}{2}$ molecules of type A arriving no later than $X_{(\frac{n+1}{2})}(i)$, and there are at most $\frac{n-1}{2}$ molecules of type B arriving no later than $X_{(\frac{n+1}{2})}(i)$. Since $\frac{n+1}{2} + \frac{n-1}{2} = n$, for the majority-vote detection, the detection results are $\hat{s}_i = 1$ and $\hat{s}_{i+1} = 0$, i.e., s_i and s_{i+1} do not switch. \square

After applying the lemma to (3.8), the BER under the majority-vote detection without background noise is given in (3.10).

$$\begin{aligned} \Pr\{\hat{s}_i^{\text{MVD}} \neq s_i\} &\approx \frac{1}{4} \Pr\left\{X_{(\frac{n+1}{2})}(i-1) > X_{(\frac{n+1}{2})}(i) + T_s \text{ or } X_{(\frac{n+1}{2})}(i) > X_{(\frac{n+1}{2})}(i+1) + T_s \right. \\ &\quad \left. \text{or } \hat{E}_{000}^{\text{MVD}} | E_{010}\right\} \\ &\quad + \frac{1}{4} \Pr\left\{X_{(\frac{n+1}{2})}(i-1) > X_{(\frac{n+1}{2})}(i) + T_s\right\} \\ &\quad + \frac{1}{4} \Pr\left\{X_{(\frac{n+1}{2})}(i) > X_{(\frac{n+1}{2})}(i+1) + T_s\right\}. \end{aligned} \quad (3.10)$$

Now we analyze the threshold-based detection algorithm. Similarly, by the assumption in Sec. 3.4.1, the BER of the threshold-based detection algorithm, denoted by $P_c^{\text{TD}}(\lambda)$, can be derived as

$$\begin{aligned} P_c^{\text{TD}}(\lambda) &= \Pr\{\hat{s}_i^{\text{TD}} \neq s_i\} \\ &\approx \frac{1}{4} \Pr\{\hat{E}_{001}^{\text{TD}}(\lambda) \cup \hat{E}_{100}^{\text{TD}}(\lambda) | E_{010}\} + \frac{1}{4} \Pr\{\hat{E}_{101}^{\text{TD}}(\lambda) | E_{011}\} + \frac{1}{4} \Pr\{\hat{E}_{101}^{\text{TD}}(\lambda) | E_{110}\}. \end{aligned} \quad (3.11)$$

Information source	0	1	0
Modulation	$\begin{matrix} \text{B} \\ \text{B B} \end{matrix}$	$\begin{matrix} \text{A} \\ \text{A A} \end{matrix}$	$\begin{matrix} \text{B} \\ \text{B B} \end{matrix}$
Possible outcome in $\widehat{E}_{001}^{\text{MVD}}$			
Received pattern	$\boxed{\text{B B B}}$	$\boxed{\text{A B B}}$	$\boxed{\text{A A B}}$
Detection result	0	0	1
Possible outcome in $\widehat{E}_{100}^{\text{MVD}}$			
Received pattern	$\boxed{\text{B A A}}$	$\boxed{\text{B B A}}$	$\boxed{\text{B B B}}$
Detection result	1	0	0
Possible outcome in $\widehat{E}_{000}^{\text{MVD}}$			
Received pattern	$\boxed{\text{B B A}}$	$\boxed{\text{B A B}}$	$\boxed{\text{A B B}}$
Detection result	0	0	0



Figure 13: Example of the events $\widehat{E}_{001}^{\text{MVD}}$, $\widehat{E}_{100}^{\text{MVD}}$, and $\widehat{E}_{000}^{\text{MVD}}$ given that the information sequence ‘0, 1, 0’ is transmitted.

If the threshold is λ , it can be observed that when $s_{i-1} \neq s_i$, the switching of s_{i-1} and s_i occurs when

$$X_{(\lambda)}(i-1) > X_{(\lambda)}(i) + T_s. \quad (3.12)$$

Therefore, (3.11) can be approximated by (3.13).

$$\begin{aligned} \Pr\{\widehat{s}_i^{\text{TD}} \neq s_i\} &\approx \frac{1}{4} \Pr\{X_{(\lambda)}(i-1) > X_{(\lambda)}(i) + T_s \text{ or } X_{(\lambda)}(i) > X_{(\lambda)}(i+1) + T_s\} \\ &\quad + \frac{1}{4} \Pr\{X_{(\lambda)}(i-1) > X_{(\lambda)}(i) + T_s\} + \frac{1}{4} \Pr\{X_{(\lambda)}(i) > X_{(\lambda)}(i+1) + T_s\} \\ &\stackrel{(a)}{=} \frac{1}{2} \Pr\{X_{(\lambda)}(i-1) > X_{(\lambda)}(i) + T_s\} + \frac{1}{2} \Pr\{X_{(\lambda)}(i) > X_{(\lambda)}(i+1) + T_s\} \\ &\quad - \frac{1}{4} \Pr\{X_{(\lambda)}(i-1) > X_{(\lambda)}(i) + T_s > X_{(\lambda)}(i+1) + 2T_s\}. \quad (3.13) \end{aligned}$$

The equality in (3.13) (denoted by ‘(a)’) results from the property $\Pr\{A \cup B\} = \Pr\{A\} + \Pr\{B\} - \Pr\{A \cap B\}$. Again, we utilize the fact that the probability of switching happening to the information bits that are more than two intervals apart is small. Then the negative term in (3.13) is negligible. Moreover, since the probability that s_i switches with s_{i+1} and the probability that s_{i-1} switches with

s_i are the same, it is given that

$$\begin{aligned}
P_c^{\text{TD}} &= \Pr\{\hat{s}_i^{\text{TD}} \neq s_i\} \\
&\approx \Pr\{X_{(\lambda)}(i-1) > X_{(\lambda)}(i) + T_s\} \\
&= \int_{-\infty}^{\infty} \Pr\{X_{(\lambda)}(i) < u - T_s | X_{(\lambda)}(i-1) = u\} f_{X_{(\lambda)}}(u) du \\
&= \int_{-\infty}^{\infty} F_{X_{(\lambda)}}(u - T_s) f_{X_{(\lambda)}}(u) du \\
&= \int_{T_s}^{\infty} F_{X_{(\lambda)}}(u - T_s) f_{X_{(\lambda)}}(u) du,
\end{aligned} \tag{3.14}$$



which can be evaluated numerically.

To compare the majority-vote detection algorithm and the threshold-based detection algorithm, we start from (3.8) and the lemma.

$$\begin{aligned}
P_c^{\text{MVD}} &\approx \frac{1}{4} \Pr\{\hat{E}_{001}^{\text{MVD}} \cup \hat{E}_{100}^{\text{MVD}} \cup \hat{E}_{000}^{\text{MVD}} | E_{010}\} + \frac{1}{4} \Pr\{\hat{E}_{101}^{\text{MVD}} | E_{011}\} + \frac{1}{4} \Pr\{\hat{E}_{101}^{\text{MVD}} | E_{110}\} \\
&= \left[\frac{1}{4} \Pr\{\hat{E}_{001}^{\text{TD}}(\lambda) \cup \hat{E}_{100}^{\text{TD}}(\lambda) \cup \hat{E}_{000}^{\text{MVD}} | E_{010}\} + \frac{1}{4} \Pr\{\hat{E}_{101}^{\text{TD}}(\lambda) | E_{011}\} \right. \\
&\quad \left. + \frac{1}{4} \Pr\{\hat{E}_{101}^{\text{TD}}(\lambda) | E_{110}\} \right]_{\lambda=\frac{n+1}{2}} \\
&\geq \left[\frac{1}{4} \Pr\{\hat{E}_{001}^{\text{TD}}(\lambda) \cup \hat{E}_{100}^{\text{TD}}(\lambda) | E_{010}\} + \frac{1}{4} \Pr\{\hat{E}_{000}^{\text{MVD}} | E_{010}\} + \frac{1}{4} \Pr\{\hat{E}_{101}^{\text{TD}}(\lambda) | E_{011}\} \right. \\
&\quad \left. + \frac{1}{4} \Pr\{\hat{E}_{101}^{\text{TD}}(\lambda) | E_{110}\} \right]_{\lambda=\frac{n+1}{2}}
\end{aligned} \tag{3.15}$$

$$\begin{aligned}
&= [P_c^{\text{TD}}(\lambda)]_{\lambda=\frac{n+1}{2}} + \frac{1}{4} \Pr\{\hat{E}_{000}^{\text{MVD}} | E_{010}\} \\
&> [P_c^{\text{TD}}(\lambda)]_{\lambda=\frac{n+1}{2}},
\end{aligned} \tag{3.16}$$

where (3.15) comes from the union bound. Therefore, we conclude that the threshold-based detection with $\lambda = \frac{n+1}{2}$ outperforms the majority-vote detection due to the extra term $\hat{E}_{000}^{\text{MVD}}$ in (3.16).

3.4.3 Analysis when Background Noise is not Negligible

To approximate the BER when background noise is not negligible, we compute the BER resulted from the crossovers and the background noise respectively, and then discuss their joint effect. Denote P_c as the BER caused by the crossover effect ($P_c = P_c^{\text{MVD}}$ or $P_c = P_c^{\text{TD}}$), P_n as the BER caused by the background noise, and

P_e as the aggregated BER. From the union bound, we have $P_e \leq P_c + P_n$. Note that we have already calculated P_c of the two algorithms in Sec. 3.4.2. The main problem of computing P_n is due to the difficulty of enumerating all the possible patterns of the arriving molecules when background noise is taken into account. However, we can approximate P_n by computing the average number of errors in a block and dividing it by the block size L .

Although the detection performed by the receiver is asynchronous, the receiver would spend LT_s (or L time slots) on average to capture all nL molecules. For both detection algorithms, observe that whenever an unintended molecule arrives at the receiver, the following received molecule pattern in the block will be right-shifted by one. When the number of unintended molecules exceeds a certain value (which will be discussed in the following paragraphs), the molecules representing the i th bit will be right shifted such that the i th detection bit will not be performed on the corresponding molecules, and thus causes a bit insertion. An example for noise effect on the threshold-based detection is shown in Fig. 12. We assume the transmitter releases molecules (AAA, AAA, BBB) to convey information bits ‘1, 1, 0’. When background noise is negligible, the received molecule pattern will follow the order as in the example. On the other hand, when background noise is not negligible, a bit insertion is produced when the receiver receives $\lambda = 3$ unintended molecules. The subsequent bits will be right shifted and the detections will become Bernoulli random trials due to the bit insertion. We denote \mathcal{T} as the time when the bit insertion occurs, then the average number of bits being influenced by the bit insertion would be $(LT_s - \mathcal{T})/T_s$, given $\mathcal{T} < LT_s$. Since the information bits 0 or 1 are sent with equal probability, P_n can be written as

$$P_n \approx \Pr\{\mathcal{T} < LT_s\} \mathbb{E}_V \left[\frac{(LT_s - \mathcal{T})/T_s}{2L} \middle| \mathcal{T} < LT_s \right] = \Pr\{V < L\} \mathbb{E}_V \left[\frac{L - V}{2L} \middle| V < L \right], \quad (3.17)$$

where we define $V = \mathcal{T}/T_s$ and the “2” in the denominator comes from the fact that detection results obtained from the shifted sequence are Bernoulli random trials. In the following, we use V^{MVD} and V^{TD} for two algorithms to represent

the normalized time when the subsequent bit sequence becomes Bernoulli random trials.

For the majority-vote detection, if the number of unintended molecules exceed $\frac{n+1}{2}$ at time G^{MVD} , there will be less than $\frac{n-1}{2}$ intended molecules in the subsequent bit detection, and hence the detection results will become Bernoulli random trials. Denote $\{N_A(t) : 0 \leq t < LT_s\}$ and $\{N_B(t) : 0 \leq t < LT_s\}$ as two random processes which respectively represent the number of unintended molecules of type A and type B arriving at the receiver from the beginning of the block to time t , we have

$$G^{\text{MVD}} = \inf \left\{ t : N_A(t) + N_B(t) \geq \frac{n+1}{2} \right\}. \quad (3.18)$$

In order to compute (3.17) for the majority-vote detection, we need the distribution of V^{MVD} in (3.18). From our system model in Sec. 3.2.2, $N_A(t)$ and $N_B(t)$ are Poisson processes with rate α . The inter-arrival times of unintended molecules thus follow exponential distribution with mean $\frac{1}{\alpha}$. It is shown in (3.18) that the bit insertion occurs when the “sum” of the number of unintended molecules reaches $(n+1)/2$, regardless of the type of the unintended molecules. Therefore, it suffices to consider the inter-arrival time of the unintended molecules with either type. The mean of inter-arrival time becomes $\frac{1}{2\alpha}$. Denote the inter-arrival time of the j -th unintended molecules as τ_j , $j \in \{1, \dots, \frac{n+1}{2}\}$. Then,

$$V^{\text{MVD}} = \frac{\tau_1 + \dots + \tau_{\frac{n+1}{2}}}{T_s}. \quad (3.19)$$

It is known that the summation of i.i.d. exponential random variables follows gamma distribution, i.e., $\text{Gamma}(\frac{n+1}{2}, 2\alpha T_s)$.

$$f_{V^{\text{MVD}}}(v) = \begin{cases} \frac{(2\alpha T_s)^{(n+1)/2}}{\Gamma(\frac{n+1}{2})} v^{(n-1)/2} e^{-(2\alpha T_s)v}, & v > 0, \\ 0, & v \leq 0. \end{cases} \quad (3.20)$$

Therefore,

$$\begin{aligned}
 P_n^{\text{MVD}} &\approx \Pr\{V^{\text{MVD}} < L\} \mathbb{E}_{V^{\text{MVD}}} \left[\frac{L - V^{\text{MVD}}}{2L} \middle| V^{\text{MVD}} < L \right] \\
 &= \int_0^L \left(\frac{L - v}{L} \right) f_{V^{\text{MVD}}}(v) dv \\
 &= \frac{1}{2\Gamma(\frac{n+1}{2})} \left[\gamma\left(\frac{n+1}{2}, 2\alpha T_s L\right) - \frac{1}{2\alpha T_s L} \gamma\left(\frac{n+3}{2}, 2\alpha T_s L\right) \right], \quad (3.21)
 \end{aligned}$$

where $\gamma(s, x)$ is the lower incomplete gamma function.

For the threshold-based detection, if the number of unintended molecules of the same type exceeds λ at time G^{TD} , a bit insertion occurs, and the subsequent detected bits become Bernoulli random trials. An example is shown in Fig. 12 that when the number of type A unintended molecules reaches $\lambda = 3$, a bit insertion occurs (in this example, bit 1), and the subsequent bits (in this example, bit 0) will be right shifted. Thus we have

$$G^{\text{TD}} = \inf \{t : N_A(t) \geq \lambda\} \wedge \inf \{t : N_B(t) \geq \lambda\}, \quad (3.22)$$

where $x \wedge y$ means the minimum of x and y . In order to compute (3.17) for the threshold-based detection, we need the distribution of V^{TD} in (3.22). Similarly, we denote the inter-arrival time between the $(j-1)$ th and j th unintended molecules of type A as $\tau_{A,j}$, $j \in \{1, \dots, \lambda\}$. Then,

$$V_A^{\text{TD}} = \frac{\tau_{A,1} + \dots + \tau_{A,\lambda}}{T_s}. \quad (3.23)$$

Similarly, the inter-arrival time between the $(j-1)$ th and j th unintended molecules of type B can be written as

$$V_B^{\text{TD}} = \frac{\tau_{B,1} + \dots + \tau_{B,\lambda}}{T_s}. \quad (3.24)$$

Therefore, both V_A^{TD} and V_B^{TD} follows Gamma($\lambda, \alpha T_s$).

$$f_{V_A^{\text{TD}}}(v) = f_{V_B^{\text{TD}}}(v) = \begin{cases} \frac{(\alpha T_s)^\lambda}{\Gamma(\lambda)} v^{\lambda-1} e^{-(\alpha T_s)v}, & v > 0, \\ 0, & v \leq 0. \end{cases} \quad (3.25)$$

Since $V^{\text{TD}} = V_A^{\text{TD}} \wedge V_B^{\text{TD}}$ from (3.22), we have

$$f_{V^{\text{TD}}}(v) = 2f_{V_A^{\text{TD}}}(v) - 2f_{V_A^{\text{TD}}}(v)F_{V_A^{\text{TD}}}(v), \quad (3.26)$$



where $F_{V_A^{\text{TD}}}(v) = \frac{1}{\Gamma(\lambda)}\gamma(\lambda, \alpha T_s v)$ is the cumulative distribution function of V^{TD} . We use the method of union bound instead of directly calculating the conditional expected value through the PDF of $V_A^{\text{TD}} \wedge V_B^{\text{TD}}$. We know that bit errors in the threshold-based detection are caused by the number of unintended molecules exceeding λ , thus by the union bound, $P_n \leq P_A + P_B$, where the errors are caused by unintended type-A, type-B molecules, respectively.

$$\begin{aligned} P_n^{\text{TD}}(\lambda) &\approx 2 \Pr\{V_A^{\text{TD}} < L\} \mathbb{E}_{V_A^{\text{TD}}} \left[\frac{L - V_A^{\text{TD}}}{2L} \mid V_A^{\text{TD}} < L \right] = \int_0^L \left(\frac{L - v}{L} \right) f_{V_A^{\text{TD}}}(v) dv \\ &= \frac{1}{\Gamma(\lambda)} \left[\gamma(\lambda, \alpha T_s L) - \frac{1}{\alpha T_s L} \gamma(\lambda + 1, \alpha T_s L) \right]. \end{aligned} \quad (3.27)$$

It can be observed that P_n^{TD} depends on parameters λ and $\alpha T_s L$. To derive relationships between P_n^{TD} and those parameters, we first take derivatives with respect to $\alpha T_s L$ with formula

$$\frac{\partial \gamma(s, x)}{\partial x} = x^{s-1} e^{-x}, \quad (3.28)$$

gives

$$\frac{\partial P_n^{\text{TD}}}{\partial(\alpha T_s L)} \approx \frac{\gamma(\lambda + 1, \alpha T_s L)}{\Gamma(\lambda)(\alpha T_s L)^2} > 0, \quad (3.29)$$

which implies P_n^{TD} is monotone with the increase of $\alpha T_s L$. On the other hand, by using the asymptotic behavior that

$$\frac{\gamma(s, x)}{x^s} \rightarrow \frac{1}{s} \text{ when } x \text{ is small}, \quad (3.30)$$

if $\alpha T_s L$ is small, (3.27) can be approximated as

$$P_n^{\text{TD}}(\lambda) \approx \frac{1}{\Gamma(\lambda)} \left[\frac{(\alpha T_s L)^\lambda}{\lambda} - \frac{1}{\alpha T_s L} \frac{(\alpha T_s L)^{\lambda+1}}{\lambda + 1} \right] = \frac{(\alpha T_s L)^\lambda}{\Gamma(\lambda + 2)}, \quad (3.31)$$

which means that P_n^{TD} becomes smaller as λ grows larger.

To compare the two algorithms under the effect of background noise for any odd number n , we note that $P_c^{\text{TD}}(\frac{n+1}{2})$ is smaller than P_c^{MVD} as discussed in Sec. 3.4.2, and in this section, by applying approximation similar to (3.31),

$$P_n^{\text{MVD}} \approx \frac{(2\alpha T_s L)^{(n+1)/2}}{2\Gamma\left(\frac{n+5}{2}\right)} \approx 2^{\frac{n-1}{2}} P_n^{\text{TD}} \left(\frac{n+1}{2} \right) > P_n^{\text{TD}} \left(\frac{n+1}{2} \right). \quad (3.32)$$

Therefore, the threshold-based detection with $\lambda = \frac{n+1}{2}$ results in lower BER than the majority-vote detection even when the background noise is considered. This again proves that the threshold-based detection can outperform the majority-vote detection.

3.4.4 Optimal Choice of Signaling Interval T_s for Threshold-based Detection

When the effect of background noise is negligibly small, we can improve the BER simply by using a larger T_s since it lowers the probability of molecular crossover. However, when the background noise is not negligible, the BER performance is no longer merited from increasing T_s . Although the crossover effect is smaller when a larger T_s is used, more unintended molecules are captured by the receiver, which in turn increases BER. The same conclusion can be made by observing (3.29) that a larger T_s results in larger P_n^{TD} . Therefore, there exists an optimal T_s given λ such that the BER is minimized. In the following, we compute the approximated optimal T_s (for a given λ) and discuss some properties that may help design the optimal threshold-based detection scheme.

To find the optimal T_s , we solve the equation

$$\frac{\partial P_e}{\partial T_s} = 0. \quad (3.33)$$

Here we assume that the union bound applied in the previous subsection is tight such that $P_e \approx P_c^{\text{TD}} + P_n^{\text{TD}}$ for the threshold-based detection and solve

$$\frac{\partial P_c^{\text{TD}}}{\partial T_s} + \frac{\partial P_n^{\text{TD}}}{\partial T_s} = 0. \quad (3.34)$$

Let us define

$$g(t) = \int_t^\infty f_{X(\lambda)}(u-t)f_{X(\lambda)}(u)du. \quad (3.35)$$

Then

$$\begin{aligned}
\frac{\partial P_c^{\text{TD}}}{\partial T_s} &\approx - \int_{T_s}^{\infty} f_{X_{(\lambda)}}(u - T_s) f_{X_{(\lambda)}}(u) du \\
&= - \int_0^{\infty} f_{X_{(\lambda)}}(u) f_{X_{(\lambda)}}(u + T_s) du \\
&= -g(t = T_s).
\end{aligned} \tag{3.36}$$



Note that $g(t)$ is the PDF of $X_{(\lambda)}(i-1) - X_{(\lambda)}(i)$, or equivalently, the difference of two samples generated i.i.d. from the order statistics $X_{(\lambda)}$. We can also calculate that

$$\frac{\partial P_n^{\text{TD}}}{\partial T_s} \approx \frac{\gamma(\lambda + 1, \alpha T_s L)}{\Gamma(\lambda) \alpha L T_s^2} \approx \frac{\lambda(\alpha L)^\lambda T_s^{\lambda-1}}{\Gamma(\lambda + 2)}, \tag{3.37}$$

where the second approximation uses (3.30) given $\alpha T_s L$ small. After combining (3.34), (3.36), and (3.37), we obtain

$$\frac{\partial P_c^{\text{TD}}}{\partial T_s} + \frac{\partial P_n^{\text{TD}}}{\partial T_s} \approx \frac{\lambda(\alpha L)^\lambda T_s^{\lambda-1}}{\Gamma(\lambda + 2)} - g(t = T_s) = 0. \tag{3.38}$$

This means that the optimal T_s can be computed by solving

$$\left. \frac{g(t)}{t^{\lambda-1}} \right|_{t=T_s} = \frac{\lambda(\alpha L)^\lambda}{\Gamma(\lambda + 2)}. \tag{3.39}$$

3.5 Numerical Results

In this section, we first compare the performances of the majority-vote detection and the threshold-based detection with different number of simultaneously released molecules and various threshold values λ when no background molecules are involved. The accuracy of the theoretical BER approximation is also shown. After that, we compare the performances of the threshold-based detection with different number of simultaneously released molecules, various threshold values, and different block sizes in the presence of background noise. The accuracy of the derived approximated optimal T_s is also confirmed.

In the simulations, information bits are sent randomly with equal probability and the background noise is assumed to be Poisson distributed. The simulation parameters are $d = 100 \mu\text{m}$, drift velocity $v = 1 \mu\text{m/s}$, diffusion constant $D =$

$2.44038 \times 10^{-11} \text{ m}^2/\text{s}$ [27]. Unless otherwise specified, the block size $L = 40$ bits, and the rate of Poisson distribution is $\alpha = 2 \times 10^{-5} \text{ s}^{-1}$.

3.5.1 Performance when Background Noise is Negligible

In Fig. 14 and Fig. 15, we compare the performance of the majority-vote detection algorithm and the proposed threshold-based detection algorithm when no background noise is presented for $n = 3$ and $n = 5$ quantity-type-modulated systems, respectively, with various values of λ . The threshold-based detection algorithm yields better performance than the majority-vote detection algorithm if a proper threshold value is chosen. We also compare the theoretical BER approximations (3.14) with the simulation results of the threshold-based detection algorithm, and show that the theoretical results match the simulation results well, especially for large T_s . From the figures, the threshold-based detection with $\lambda = (n + 1)/2$ is shown to outperform the majority-vote detection, as proved in Sec. 3.4.2. Moreover, for the threshold-based detection, a smaller λ leads to better performance, and choosing $\lambda = 1$ yields the lowest BER. This is because a symbol will be error-free if less than $n - \lambda$ crossovers occur. Therefore, the value $n - \lambda$ can represent the ISI-resisting capability, and a larger $n - \lambda$ value improves the system performance. As shown in the figures, for a fixed n , choosing a smaller λ , and hence a larger $n - \lambda$, yields better performance. Thus, by applying the threshold-based detection with $\lambda \leq (n + 1)/2$, it can always achieve better performance than the majority-vote detection.

Fig. 16 summarizes the performance comparison of the majority-vote detection algorithm and the threshold-based detection algorithm when no background noise is presented. The system with type modulation, which is equivalent to the quantity-type-modulated system with $n = 1$, is also shown. It can be seen that the performance of the $n = 3$ quantity-type-modulated system with the majority-vote detection is worse than the type-modulated system when T_s is large. This shows that using a detection algorithm not tailored for the diffusion channel would nullify the benefits getting from releasing n molecules at a time. By applying the

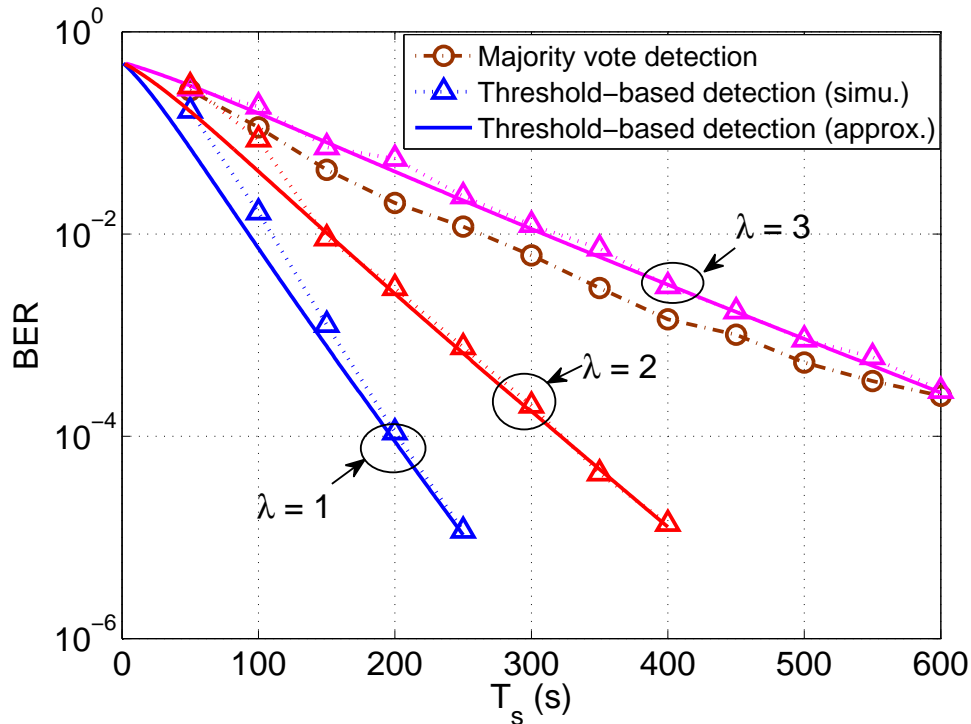


Figure 14: Performance comparison between the majority-vote detection and the proposed threshold-based detection for the $n = 3$ quantity-type-modulated system without background noise. The theoretical analysis and the simulation results are also compared.

threshold-based detection, the BER reaches 10^{-5} with less than a half of T_s compared with using the majority-vote detection. A better performance is achieved if more molecules are released at a time, i.e., with a larger n .

3.5.2 Performance when Background Noise is not Negligible

From Fig. 17 to Fig. 20, we evaluate the performance of majority-vote detection and threshold-based detection algorithms with various threshold values and block sizes under the influence of background noise. Fig. 21 further shows how the number of simultaneously released molecules affects the system performance.

In Fig. 17 and Fig. 18, we compare the performances of majority-vote detection and threshold-based detection algorithms in $n = 3$ and $n = 5$ quantity-type-modulated systems, respectively, under background noise. It can be observed that when T_s is small, a smaller λ is preferred since the BER caused by crossovers

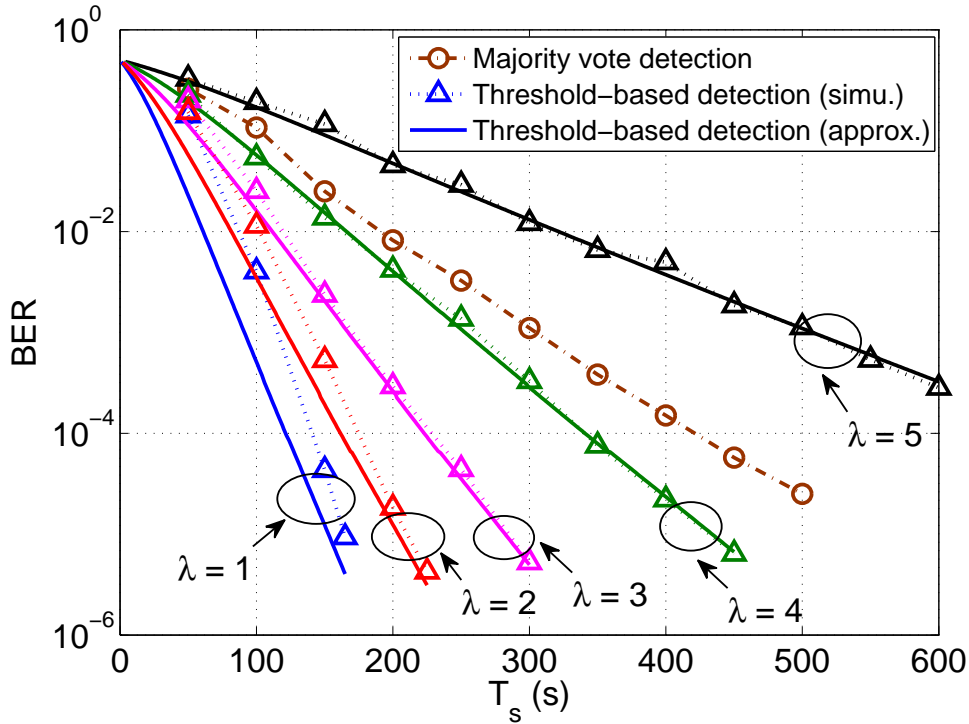


Figure 15: Performance comparison between the majority-vote detection and the proposed threshold-based detection for the $n = 5$ quantity-type-modulated system without background noise. The theoretical analysis and the simulation results are also compared.

is dominant. However, when T_s is large, systems with larger λ have better performance since they are more robust to the background noise, which is supported by (3.31). The figures also show that when $\lambda = (n+1)/2$, the BER of the threshold-based detection is lower than that of the majority-vote detection for any given T_s , which is proved in Sec. 3.4.3. This guarantees the performance of the threshold-based detection, and note that further improvements can be achieved by choosing a proper λ and T_s . The optimal T_s 's derived from (3.39) with respect to λ are also shown in the figures, which match the simulation results very well.

Fig. 19 and Fig. 20 show the BER performances of the $n = 3$ and $n = 5$ quantity-type-modulated systems under different block sizes. It can be observed that the block size affects the BER significantly for both the majority-vote detection and the threshold-based detection. The performance is better with smaller L since the ISI is mitigated by a time separation of $2T_s$ between blocks. Smaller L also reduces the amount of unintended molecules being captured by the receiver.

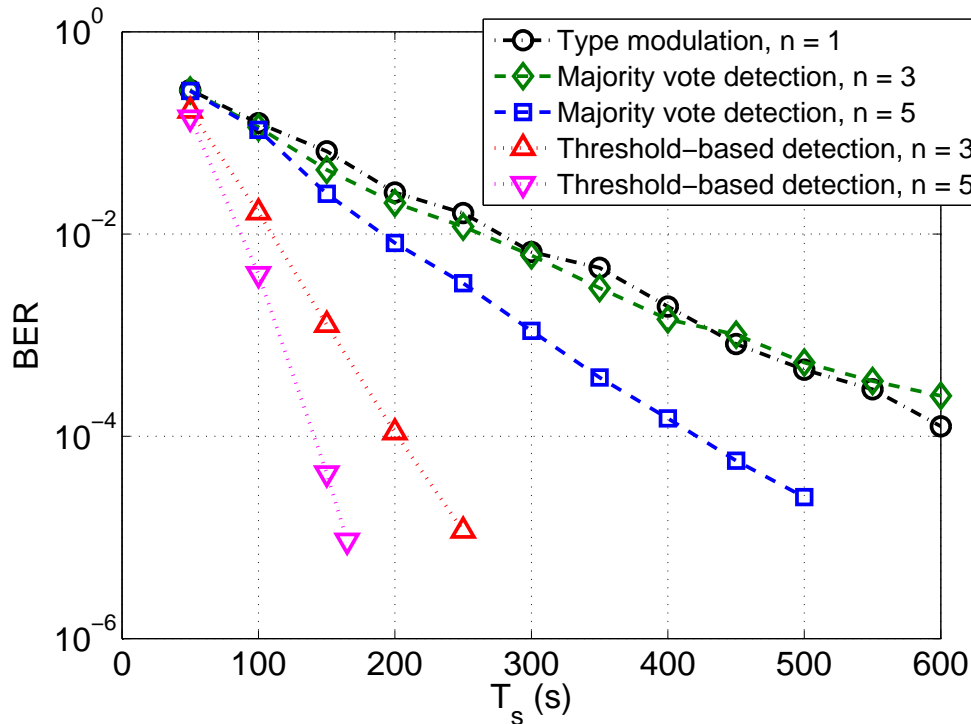


Figure 16: Performance comparison of quantity-type-modulated systems without background noise with different n (the number of molecules released at a time) and different detection algorithms. The case of $n = 1$ corresponds to the type-modulated system. $\lambda = 1$ for the threshold-based detection algorithm.

The benefits brought from smaller L can be observed from (3.29). To conclude, both the ISI effect and the background noise are small when L is small.

In Fig. 21, we summarize the performance comparison between the majority-vote detection algorithm and the threshold-based detection algorithm when the background noise is considered. Performance of the type-modulated system is also shown. It is observed that the BER of the quantity-type-modulated system with the majority-vote detection is lower than that of the type-modulated system, but is still larger than 10^{-2} . In the case of using the threshold-based detection, by choosing a proper λ and a large n , the BER is improved to 10^{-4} .

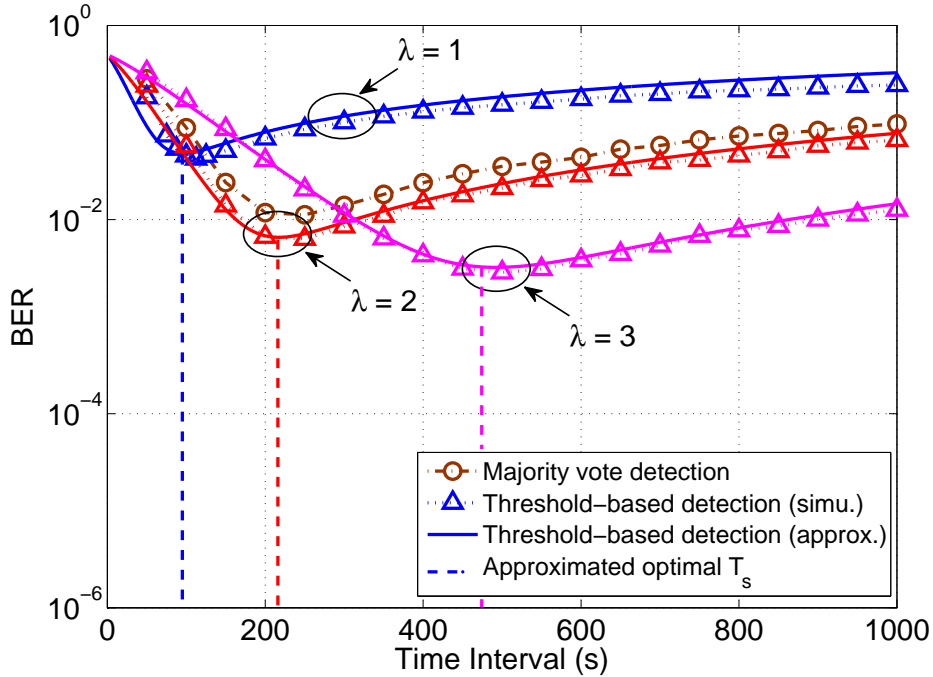


Figure 17: Performance comparison between the majority-vote detection and the proposed threshold-based detection for the $n = 3$ quantity-type-modulated system with background noise. The theoretical analysis and the simulation results are also compared.

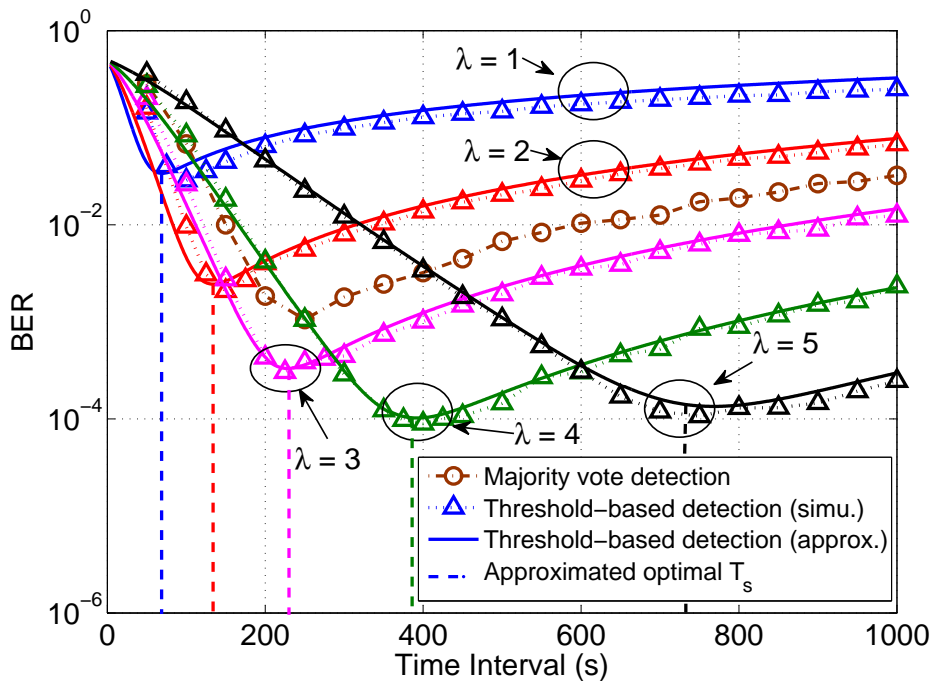


Figure 18: Performance comparison between the majority-vote detection and the proposed threshold-based detection for the $n = 5$ quantity-type-modulated system with background noise. The theoretical analysis and the simulation results are also compared.

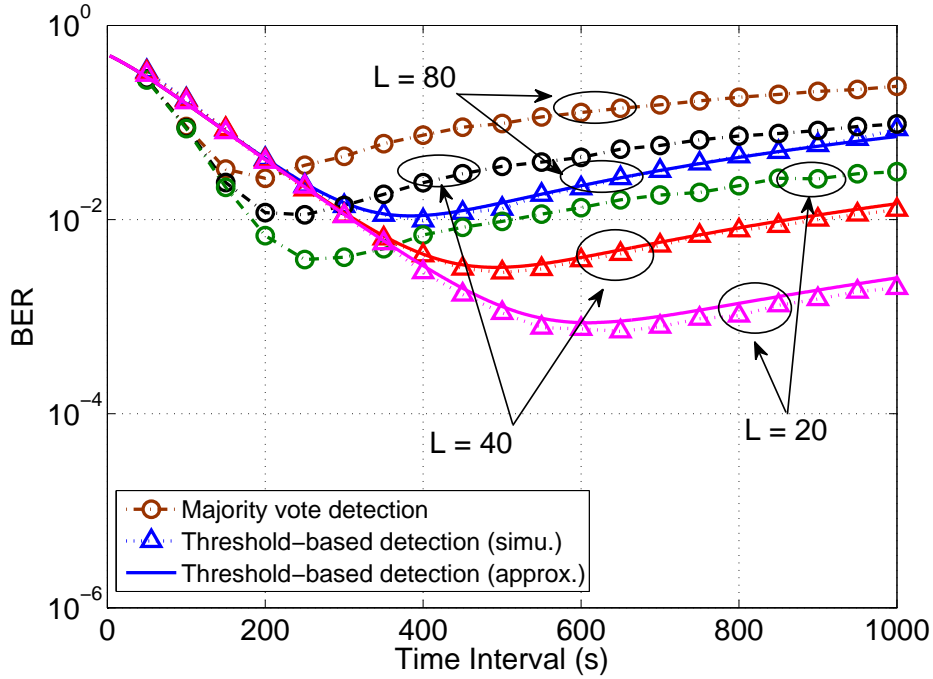


Figure 19: Performance comparison between the majority-vote detection and the proposed threshold-based detection for the $n = 3$ quantity-type-modulated system with background noise under different block sizes. The theoretical analysis and the simulation results are also compared. $\lambda = 3$.

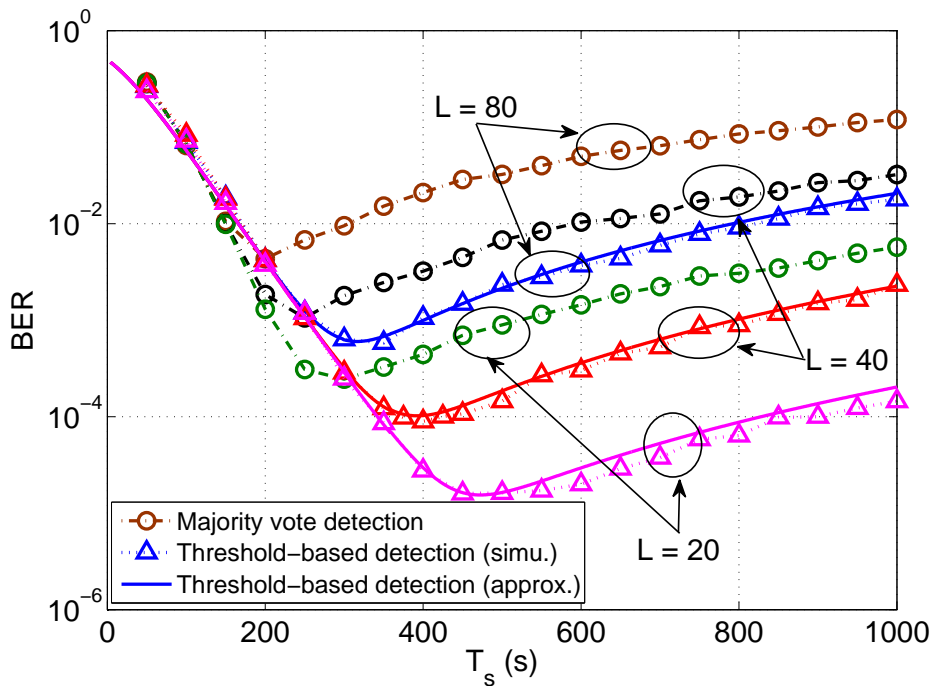


Figure 20: Performance comparison between the majority-vote detection and the proposed threshold-based detection for the $n = 5$ quantity-type-modulated system with background noise under different block sizes. The theoretical analysis and the simulation results are also compared. $\lambda = 5$.

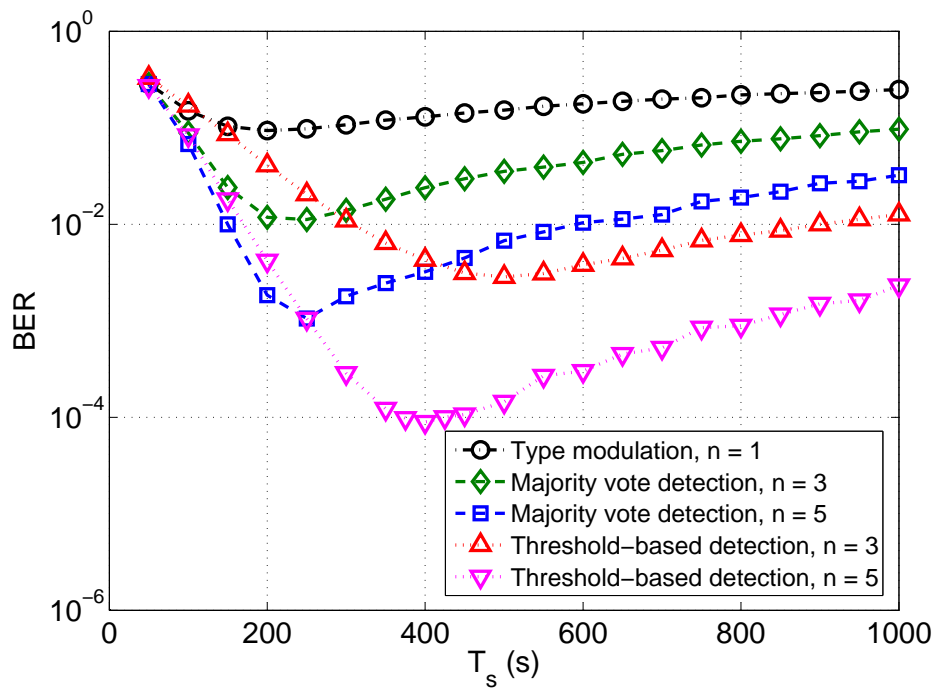


Figure 21: Performance comparison of quantity-type-modulated systems with different n using different detection algorithms in the presence of background noise. The case of $n = 1$ corresponds to the type-modulated system. $\lambda = 3$ for the $n = 3$ quantity-type-modulated system and $\lambda = 5$ for the $n = 5$ quantity-type-modulated system. $L = 40$ bits.

CHAPTER 4



WAVEFORM MODULATION

4.1 Introduction

The last two chapters mainly discussed communications schemes in coherent molecular communication, which assumes the receiver RN to be able to capture molecules one by one. Under the assumption, the channel model can be simplified by only describing the distribution of the molecule first-hitting time when a molecule arrives at RN. Practically, however, nano-machines may only sense the concentration level within a small volume around them, and hence RN may lose the information about the arriving of a single molecule. Moreover, coherent molecular communication limits possible methods to transmit bit information. Therefore, a new stochastic model is needed in order to diversify possible modulation schemes. In this chapter, we will discuss how to mathematically model the diffusion channel when continuous waveform (rather than impulse) is used to convey information. Since the work is still in its early stage, we focus waveform modulation mainly on two kinds of well-known modulation: amplitude modulation and pulse-position modulation.

4.2 System Model

4.2.1 Transmitter and Receiver Modeling

We consider two nanomachines, one transmitter nanomachine (TN) and one receiver nanomachine (RN), located in a three-dimensional Euclidean space filled with fluid medium. TN is located at $\mathbf{0}$ and RN is located at \mathbf{r} . We assume TN and RN have very small sizes compared with the distance between them. RN can sense the concentration level in the sensing region $S = \{\mathbf{x} : |\mathbf{r} - \mathbf{x}| \leq \rho\}$. For simplicity, we denote $r = |\mathbf{r}|$ to be the distance between TN and RN; $V = m(S)$

to be the measure (or volume in Euclidean space) of the sensing region.

4.2.2 Diffusion Channel Modeling

According to Fick's second law, the concentration level $U(\mathbf{r}, t)$ can be characterized by

$$\frac{\partial U}{\partial t} = D\nabla^2 U, \quad (4.1)$$

where D is the diffusion coefficient depending on the fluid medium. The results from [Jiun-Ting and Yun-Feng], which take into account the random effect of diffusion process, show that if N molecules are released simultaneously by TN at $t = 0$, the sensed concentration level at RN, denoted by $Q(\mu, N, t)$ in this thesis, is a Gaussian process with mean function $\frac{N}{V}p(t)$, where

$$p(t) = \int_S \frac{1}{(4\pi Dt)^{\frac{3}{2}}} \exp\left(-\frac{|\mathbf{x}|^2}{4Dt}\right) d\mathbf{x}, \quad (4.2)$$

The variance function is $\frac{N}{V^2}p(t)(1 - p(t))$, and the covariance function is given by

$$\begin{aligned} & \text{Cov}(Q(\mu, N, t_1), Q(\mu, N, t_2)) \\ &= \frac{N}{V^2} \left[\int_S \int_S (4\pi D(t_2 - t_1))^{-\frac{3}{2}} (4\pi D(t_1 - \tau))^{-\frac{3}{2}} \right. \\ & \quad \times \exp\left(-\frac{|\mathbf{x}_2 - \mathbf{x}_1|^2}{4D(t_2 - t_1)}\right) \exp\left(-\frac{|\mathbf{x}_1|^2}{4D(t_1 - \tau)}\right) d\mathbf{x}_2 d\mathbf{x}_1 - p(t_1 - \tau)p(t_2 - \tau) \left. \right] \end{aligned} \quad (4.3)$$

Since the volume V is only a scaling factor, it is set to be $V = 1$ in the following.

In order to make the communication system physically realizable, we cannot only consider the case that TN releases some molecules at a time instant since it requires infinite emission rate. In this study, we consider TN releases molecules with finite rate $s(t)$ in time interval $[0, T_s)$. The received number of molecules at RN is denoted by $r(\mu, t)$. The structure of the diffusion model is given in Fig. 22.

In the following, we aim at deriving the form of $r(\mu, t)$. As shown in Fig. 23, during an infinitesimal time duration $[\tau, \tau + \Delta\tau)$, $s(\tau)\Delta\tau$ molecules are released by TN. By the above results, the received number of molecules at time t is the sum of i.i.d. Gaussian random variables given by

$$r(\mu, t) = \lim_{\Delta\tau \rightarrow 0} \sum_{\tau} Q(\mu, s(\tau)\Delta\tau, t - \tau). \quad (4.4)$$

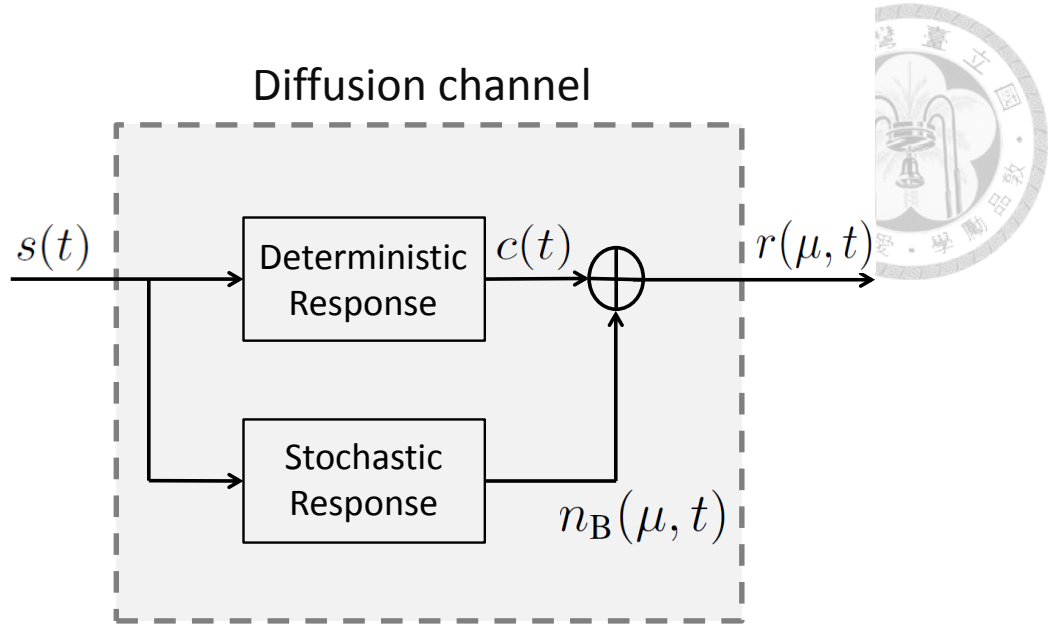


Figure 22: Proposed diffusion model for molecular communication in a fluid medium.

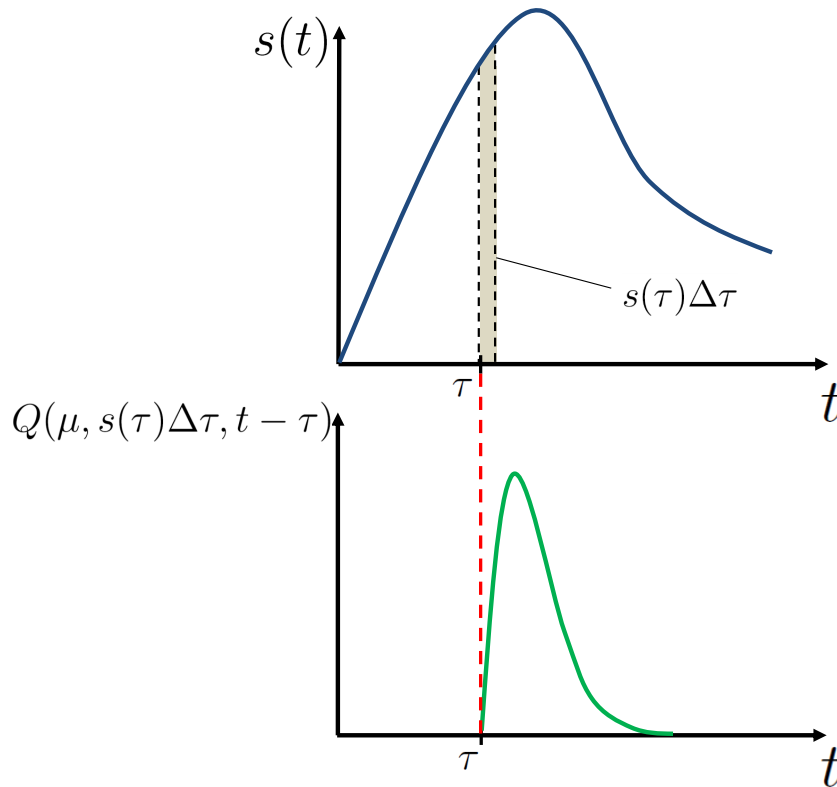


Figure 23: Channel response results from an infinitesimal duration of transmitted signal $s(t)$.

Therefore, $r(\mu, t)$ has Gaussian distribution and has mean

$$\begin{aligned} E[r(\mu, t)] &= \lim_{\Delta\tau \rightarrow 0} \sum_{\tau} E[Q(\mu, s(\tau)\Delta\tau, t - \tau)] \\ &= \lim_{\Delta\tau \rightarrow 0} \sum_{\tau} s(\tau)\Delta\tau p(t - \tau) = \int_0^{T_s} p(t - \tau)s(\tau)d\tau = s(t) \star p(t). \quad (4.5) \end{aligned}$$

and variance

$$\begin{aligned}
\text{Var}(r(\mu, t)) &= \lim_{\Delta\tau \rightarrow 0} \sum_{\tau} \text{Var}(Q(\mu, s(\tau)\Delta\tau, t - \tau)) \\
&= \lim_{\Delta\tau \rightarrow 0} \sum_{\tau} s(\tau)\Delta\tau p(t - \tau)(1 - p(t - \tau)) \\
&= \int_0^{T_s} s(\tau)p(t - \tau)(1 - p(t - \tau))d\tau \\
&= s(t) \star [p(t)(1 - p(t))].
\end{aligned} \tag{4.6}$$



As a consequence, the received signal $r(\mu, t)$ at RN can be viewed as the sum of two responses: $c(t)$ from a linear part and $n_B(\mu, t)$ from a random part of the channel, i.e.

$$r(\mu, t) = c(t) + n_B(\mu, t), \tag{4.7}$$

where

$$c(t) = s(t) \star p(t), \tag{4.8}$$

and $n_B(\mu, t)$ is a zero mean Gaussian process with variance function

$$\text{Var}(n_B(\mu, t)) = s(t) \star [p(t)(1 - p(t))]. \tag{4.9}$$

Intuitively speaking, $c(t)$ is the mean concentration sensed by RN, and $n_B(\mu, t)$ is the noise results from Brownian motion.

In order to obtain reliable detection, sometimes we need the covariance of the received signal at two time instants t_1 and t_2 .

$$\begin{aligned}
\text{Cov}(r(\mu, t_1), r(\mu, t_2)) &= \text{Cov}\left(\sum_{\tau_1} Q(\mu, s(\tau_1)\Delta\tau_1, t_1 - \tau_1), \sum_{\tau_2} Q(\mu, s(\tau_2)\Delta\tau_2, t_2 - \tau_2)\right) \\
&= \sum_{\tau} \text{Cov}(Q(\mu, s(\tau)\Delta\tau, t_1 - \tau), Q(\mu, s(\tau)\Delta\tau, t_2 - \tau)) \\
&= \int_0^{T_s} s(\tau) \left[\int_S \int_S (4\pi D(t_2 - t_1))^{-\frac{3}{2}} (4\pi D(t_1 - \tau))^{-\frac{3}{2}} \right. \\
&\quad \times \exp\left(-\frac{|\mathbf{x}_2 - \mathbf{x}_1|^2}{4D(t_2 - t_1)}\right) \exp\left(-\frac{|\mathbf{x}_1|^2}{4D(t_1 - \tau)}\right) d\mathbf{x}_2 d\mathbf{x}_1 \\
&\quad \left. - p(t_1 - \tau)p(t_2 - \tau) \right] d\tau.
\end{aligned} \tag{4.10}$$

The above equation can also be interpreted as the autocorrelation function of the noise $n_B(\mu, t)$. We apply the following theorem to check the consistency between (4.9) and (4.10).

Theorem 1. *In \mathbb{R}^d space, K_t with the form*

$$K_t(\mathbf{x}) = \frac{1}{(4\pi t)^{d/2}} \exp\left(-\frac{|\mathbf{x}|^2}{4t}\right), \quad (4.11)$$

is an approximation to the identity. Therefore, for any given $\varphi \in L^1(\mathbb{R}^d)$, we have

$$K_t \star \varphi(\mathbf{x}) \rightarrow \varphi(\mathbf{x}) \text{ for a.e. } \mathbf{x} \in \mathbb{R}^d. \quad (4.12)$$

Theorem 2. *For any given measurable set $S \subset \mathbb{R}^d$ and $\varphi \in L^1(\mathbb{R}^d)$,*

$$\int_S K_t(\mathbf{x}_2 - \mathbf{x}_1) \varphi(\mathbf{x}_1) d\mathbf{x}_1 \rightarrow \varphi(\mathbf{x}_2) \text{ for a.e. } \mathbf{x}_2 \in S. \quad (4.13)$$

Proof. It is clear that $\varphi \mathbb{1}_S \in L^1(\mathbb{R}^d)$. Apply Theorem 1, we have

$$\begin{aligned} & \int_S K_t(\mathbf{x}_2 - \mathbf{x}_1) \varphi(\mathbf{x}_1) d\mathbf{x}_1 \\ &= \int_{\mathbb{R}^d} K_t(\mathbf{x}_2 - \mathbf{x}_1) \varphi(\mathbf{x}_1) \mathbb{1}_S(\mathbf{x}_1) d\mathbf{x}_1 \\ &= K_t \star (\varphi \mathbb{1}_S)(\mathbf{x}_2) \\ &\rightarrow \varphi \cdot \mathbb{1}_S(\mathbf{x}_2) \text{ for a.e. } \mathbf{x}_2 \in \mathbb{R}^d. \end{aligned} \quad (4.14)$$

For $\mathbf{x}_2 \in S$, $\varphi \cdot \mathbb{1}_S(\mathbf{x}_2) = \varphi(\mathbf{x}_2)$, and hence completed the proof. \square

By setting $d = 3$ and

$$K_{D(t_2-t_1)}(\mathbf{x}) = (4\pi D(t_2 - t_1))^{-\frac{3}{2}} \exp\left(-\frac{|\mathbf{x}|^2}{4D(t_2 - t_1)}\right), \quad (4.15)$$

and under the case that $t_2 \rightarrow t_1^+$, (4.10) becomes

$$\lim_{t_2 \rightarrow t_1^+} \text{Cov}(r(\mu, t_1), r(\mu, t_2)) = \int_0^{T_s} s(\tau) p(t_1 - \tau) [1 - p(t_1 - \tau)] d\tau, \quad (4.16)$$

which in turn shows the consistency. Moreover, it is shown that $n_B(\mu, t)$ is a non-white process. In the following, we denote the autocorrelation function of n_B by $R_{n_B}(t_1, t_2)$.

4.3 Signal Modulation and Detection

Assume a signal set $\{s_i(t)\}_{i=0}^1 \subset L^2([0, T_s])$ is used to transmit binary information '0' and '1'. $s_0(t)$ and $s_1(t)$, which represent molecule releasing rate of TN at time t , are transmitted with equal probability. After the signal $s_i(t)$ passes through the diffusion channel, the received waveform $r(\mu, t)$ at RN is defined on $[0, \infty)$. Since it is not practical and not possible to detect a single bit by observing an infinite duration of time, the observation duration is assumed to be constrained in a bounded interval $[0, T)$ in this study. In the following, we aim at designing detection schemes at RN. One major problem comes from the observation that the statistical behaviors of the noise, which are characterized in (4.9) and (4.10), are determined by the transmitted signal $s_i(t)$. Details about the problem will be presented in the following paragraph. For convenience, we use $R_{n_{B,i}}(t_1, t_2)$, to denote the autocorrelation function of $n_{B,i}(\mu, t)$, where $i \in \{0, 1\}$ represents the transmitted bit.

Common approach to solve detection problems is to apply likelihood ratio test based on a finite-length observation vector obtained from the received signal. In order to apply classical likelihood ratio test, we first transform the received continuous waveform in (4.7) to a finite sequence of random variables, which is denoted as

$$\mathbf{r} = [r_1 \cdots r_K]^\top. \quad (4.17)$$

The observation vector \mathbf{r} can be obtained by either sampling the original waveform or expanding the waveform onto a set of orthonormal basis. Although when $K \rightarrow \infty$, both approaches contain sufficient information about the received continuous process, it is not the case for a finite K . For a finite valued K , correlated random variables are obtained by sampling the original waveform while uncorrelated random variables can be obtained by orthogonal expansion, e.g., Karhunen-Loève (KL) expansion. Intuitively, K random variables should be uncorrelated; otherwise, the effective number of observation would be less than K . Therefore, orthogonal expansion is of our main focus in this study, and the sample-based

approach is served as a benchmark design method.

From KL expansion, each element in \mathbf{r} is represented by

$$r_k(\mu) = \int_0^T r(\mu, t) \phi_k(t) dt, \quad k = 1, 2, \dots, K, \quad (4.18)$$

where each $\phi_k \in L^2([0, T])$ is a solution to the integral equation

$$\int_0^T R_{n_B, i}(t, s) \phi_k(s) ds = \lambda_k \phi_k(t). \quad (4.19)$$

One major problem is that the set of solutions $\{\phi_k(t)\}_{k=1}^K$ should satisfy (4.19) for both $i = 0$ and $i = 1$. In [28], the author showed that it is possible to solve for a set of basis functions which enables simultaneous orthogonal expansion. However, the examples provided in [28] were on special autocorrelation functions, and the method is mathematically hard to generalize. In this study, instead of solving (4.19) for all $R_{n_B, i} \in L^2$, we limit possible $R_{n_B, i}$ by using special modulations, i.e., amplitude modulation and pulse position modulation.

By amplitude modulation, we mean that for $t \in [0, T_s)$,

$$\frac{s_0(t)}{s_1(t)} = C, \quad (4.20)$$

where C is a constant. From (4.10), for $(t_1, t_2) \in [0, \infty) \times [0, \infty)$ we have

$$\frac{R_{n_B, 0}(t_1, t_2)}{R_{n_B, 1}(t_1, t_2)} = C. \quad (4.21)$$

Therefore, if the set of solutions $\{\phi_k(t)\}_{k=1}^K$ satisfies (4.19) for $i = 1$ in the way

$$\int_0^T R_{n_B, 1}(t, s) \phi_k(s) ds = \lambda_k \phi_k(t), \quad (4.22)$$

the equation also holds for

$$\int_0^T R_{n_B, 0}(t, s) \phi_k(s) ds = C \lambda_k \phi_k(t). \quad (4.23)$$

To form a likelihood ratio test, it can be shown that

$$\mathbf{r} | s_0(t) \sim \mathcal{N}(\mathbf{c}_0, \mathbf{\Sigma}_0), \quad (4.24)$$

$$\mathbf{r} | s_1(t) \sim \mathcal{N}(\mathbf{c}_1, \mathbf{\Sigma}_1), \quad (4.25)$$



where \mathbf{c}_0 and \mathbf{c}_1 are obtained by expanding $c_0(t)$ and $c_1(t)$ onto $\{\phi_k(t)\}_{k=1}^K$. Moreover,

$$\mathbf{\Sigma}_0 = C \cdot \text{diag}\{\lambda_1, \dots, \lambda_K\}, \quad (4.26)$$

$$\mathbf{\Sigma}_1 = \text{diag}\{\lambda_1, \dots, \lambda_K\}. \quad (4.27)$$

By pulse position modulation, we mean $s_0(t)$ and $s_1(t)$ occupy disjoint subspaces in time domain to bear information, i.e.,

$$\text{supp}(s_0) \cap \text{supp}(s_1) = \emptyset. \quad (4.28)$$

Specifically, we choose $s_0(t)$ to occupy $[0, T_s/2)$ and $s_1(t)$ to occupy $[T_s/2, T_s)$, hoping $c_0(t)$ and $c_1(t)$ could have disjoint supports $[0, T_s/2)$ and $[T_s/2, T_s)$, such that $c_0(t)$ and $c_1(t)$ also occupy disjoint subspaces. According to the results in [29], when signals occupy disjoint subspaces, simultaneous orthogonal expansion can be achieved. However, since the channel response $p(t)$ is IIR,

$$\text{supp}(c_0) \cap \text{supp}(c_1) \neq \emptyset, \quad (4.29)$$

which means the requirement to apply [29] is not satisfied. More precisely, when $s_0(t)$ is transmitted, $c_0(t)$ sensed by RN has components $[T_s/2, T_s)$, which is occupied by $c_1(t)$. On the other hand, when $s_1(t)$ is transmitted, $c_1(t)$ do not have any component lying on $[0, T_s/2)$. In this study, we use $K/2$ basis functions $\{\phi_k^0\}_{k=1}^{K/2}$ to expand the received waveform in $[0, T_s/2)$ and $\{\phi_k^1\}_{k=1}^{K/2}$ are used to expand the received waveform in $[T_s/2, T_s)$. Combining the two sets of basis functions results in

$$\{\phi_1^0, \dots, \phi_{\frac{K}{2}}^0, \phi_1^1, \dots, \phi_{\frac{K}{2}}^1\}, \quad (4.30)$$

which is used to obtain totally K observations. When either $s_0(t)$ or $s_1(t)$ is transmitted, K observations can be obtained by RN and at least $K/2$ of them are uncorrelated. To form a likelihood ratio test, it can be shown that

$$\mathbf{r}|s_0(t) \sim \mathcal{N}(\mathbf{c}_0, \mathbf{\Sigma}_0), \quad (4.31)$$

$$\mathbf{r}|s_1(t) \sim \mathcal{N}(\mathbf{c}_1, \mathbf{\Sigma}_1). \quad (4.32)$$

Moreover,

$$\Sigma_0 = \begin{bmatrix} \Lambda_0 & \Delta_{01} \\ \Delta_{10} & \Lambda_{11} \end{bmatrix}, \quad (4.33)$$

$$\Sigma_1 = \begin{bmatrix} \mathbf{0} & \mathbf{0} \\ \mathbf{0} & \Lambda_1 \end{bmatrix}, \quad (4.34)$$



where $\Lambda_i = \text{diag}\{\lambda_1^i, \dots, \lambda_{K/2}^i\}$, $i \in \{0, 1\}$ consists of eigenvalues solved from

$$\int_0^{\frac{T}{2}} R_{n_B,0}(t, s) \phi_k^0(s) ds = \lambda_k^0 \phi_k^0(t), \quad (4.35)$$

$$\int_{\frac{T}{2}}^T R_{n_B,1}(t, s) \phi_k^1(s) ds = \lambda_k^1 \phi_k^1(t). \quad (4.36)$$

Δ_{ij} is given by

$$[\Delta_{ij}]_{mn} = \int \int R_{n_B,0}(t, s) \phi_m^i(t) \phi_n^j(s) dt ds. \quad (4.37)$$

Finally, the decision rule for amplitude modulation and pulse-position modulation derived from likelihood ratio test is given by

$$(\mathbf{r} - \mathbf{c}_1)^\top \Sigma_1^{-1} (\mathbf{r} - \mathbf{c}_1) - (\mathbf{r} - \mathbf{c}_0)^\top \Sigma_0^{-1} (\mathbf{r} - \mathbf{c}_0) \underset{H_1}{\overset{H_0}{\geq}} \ln \frac{|\Sigma_0|}{|\Sigma_1|}. \quad (4.38)$$

In the following, we aim at solving (4.19) on $[T_I, T_F)$. For amplitude modulation, $[T_I, T_F) = [0, T)$. For pulse-position modulation, $[T_I, T_F) = [0, T_s/2)$ for $i = 0$ and $[T_I, T_F) = [T_s/2, T_s)$ for $i = 1$. To simplify the notation, we drop the subscript of $R_{n_B,i}(t_1, t_2)$ and the total number of basis functions is denoted by N . For amplitude modulation, $N = K$, and for pulse-position modulation, $N = K/2$. The form for $R(t_1, t_2)$ is given in (4.10), which is mathematically hard to use. We apply the following theorem to approximate $R(t_1, t_2)$ by a separable function.

Theorem 3. *Let \mathcal{H}_1 and \mathcal{H}_2 be Hilbert spaces and let A be a compact operator from \mathcal{H}_1 into \mathcal{H}_2 . Then*

$$A = \sum_{n=1}^{\infty} \tilde{\lambda}_n (f_n \otimes g_n), \quad (4.39)$$

with

1. $\{\tilde{\lambda}_n^2\}$ the non-zero eigenvalues of A^*A and AA^* ,

2. $\{g_n\}$ orthonormal eigenfunctions of A^*A ,
3. $\{f_n\}$ orthonormal eigenfunctions of AA^* satisfying $Ag_n = \tilde{\lambda}_n f_n$.

The above is known as the singular value expansion (SVE) of A . In [30], the author proposed how to compute approximation to SVE of compact operators by universal methods. Let $\{\psi_n(t)\}_{n=1}^N, T_I \leq t < T_F$ be the set of basis functions. Define matrix $\mathbf{A} = [a_{nm}]$,

$$a_{nm} = \int_{T_I}^{T_F} \int_{T_I}^{T_F} R(s, t) \psi_n(s) \psi_m(t) ds dt. \quad (4.40)$$

\mathbf{A} is symmetric since

$$\begin{aligned} a_{mn} &= \int_{T_I}^{T_F} \int_{T_I}^{T_F} R(s, t) \psi_m(s) \psi_n(t) ds dt \\ &= \int_{T_I}^{T_F} \int_{T_I}^{T_F} R(t, s) \psi_n(t) \psi_m(s) dt ds \\ &= a_{nm}. \end{aligned} \quad (4.41)$$

Therefore, the singular value decomposition (SVD) of \mathbf{A} can be written as

$$\mathbf{A} = \mathbf{U} \tilde{\Lambda} \mathbf{U}^\top = \sum_{n=1}^N \tilde{\lambda}_n \mathbf{u}_n \mathbf{u}_n^\top, \quad (4.42)$$

we can approximate $R(t_1, t_2)$ confined in $[T_I, T_F] \times [T_I, T_F]$ by SVE as

$$R(t_1, t_2) \approx \hat{R}(t_1, t_2) = \sum_{n=1}^N \tilde{\lambda}_n f_n(t_1) f_n(t_2), \quad (4.43)$$

where

$$f_n(t) = \sum_{m=1}^N u_{mn} \psi_m(t), \quad (4.44)$$

We then apply the approximation in (4.43) to solve the alternative form of (4.19):

$$\int_{T_I}^{T_F} \hat{R}(t, s) \phi_k(s) ds = \lambda_k \phi_k(t), \quad (4.45)$$

which gives

$$\begin{aligned} \lambda_k \phi_k(t) &= \int_{T_I}^{T_F} \left[\sum_{n=1}^N \tilde{\lambda}_n f_n(t) f_n(s) \right] \phi_k(s) ds \\ &= \sum_{n=1}^N \tilde{\lambda}_n f_n(t) \left[\int_{T_I}^{T_F} f_n(s) \phi_k(s) ds \right]. \end{aligned} \quad (4.46)$$

Writing

$$c_n = \int_{T_1}^{T_F} f_n(y) \phi_k(s) ds, \quad (4.47)$$

ϕ_k is of the form

$$\phi_k(t) = \frac{1}{\lambda_k} \sum_{n=1}^N c_n \tilde{\lambda}_n f_n(x). \quad (4.48)$$

By letting matrix $\mathbf{B} = [b_{nm}]$ with

$$b_{nm} = \int_{T_1}^{T_F} \tilde{\lambda}_m f_m(x) f_n(x) dx = \tilde{\lambda}_m \mathbf{u}_m^\top \mathbf{u}_n = \tilde{\lambda}_m \delta_{mn}, \quad (4.49)$$

and vector $\mathbf{c} = [c_1 \cdots c_N]^\top$, we can solve non-zero \mathbf{c} from

$$(\mathbf{B} - \lambda_k \mathbf{I}) \mathbf{c} = \mathbf{0}. \quad (4.50)$$

The solution pairs (λ_k, \mathbf{c}) to (4.50) are given by $\{(\tilde{\lambda}_n, \mathbf{e}_n)\}_{n=1}^N$. By substituting the solutions into (4.48), it is shown that the set of orthonormal basis functions is

$$\{\phi_k(t)\}_{k=1}^N = \{f_n(t)\}_{n=1}^N. \quad (4.51)$$

Since the set of basis functions is derived from (4.45) but not (4.19), it is required to check whether the components of the observation vector are uncorrelated in order to guarantee N effective observations. When the received signal $r(t)$ is expanded to \mathbf{r} by (4.51), the correlation between components is given by

$$\begin{aligned} \text{Cov}([\mathbf{r}]_n, [\mathbf{r}]_m) &= \int_{T_1}^{T_F} \int_{T_1}^{T_F} R(s, t) f_n(s) f_m(t) ds dt \\ &= \sum_{i,j} u_{in} u_{jm} \int_{T_1}^{T_F} \int_{T_1}^{T_F} R(s, t) \psi_n(s) \psi_m(t) ds dt \\ &= \sum_{i,j} u_{in} u_{jm} a_{ij} \\ &= \lambda_n \delta_{nm}, \end{aligned} \quad (4.52)$$

which shows the components of \mathbf{r} are mutually uncorrelated.

4.4 Numerical Results

In this section, we compare the BER performance for the two detection methods: sampling-based detection and expansion-based detection performed on amplitude modulation and pulse-position modulation. The set of universal basis



functions used in (4.40) is chosen to be

$$\psi_n(t) = \frac{1}{\sqrt{\Delta t}} \cdot \mathbb{1}_{\{(n-1)\Delta t \leq t < n\Delta t\}}(t). \quad (4.53)$$

with

$$\Delta t = \frac{T_F - T_I}{N}. \quad (4.54)$$

being the width of each function.

In the simulations, information bits ‘0’ and ‘1’ are sent with equal probability. One-shot transmission is assumed since we focus on the efficiency of observations made by sample-based detection and expansion-based detection. Unless otherwise specified, the parameters are set to $r = 3 \mu\text{m}$, $d = 100 \mu\text{m}$, $D = 10^4 \mu\text{m}^2/\text{sec}$, and $T_s = 10 \text{ sec}$.

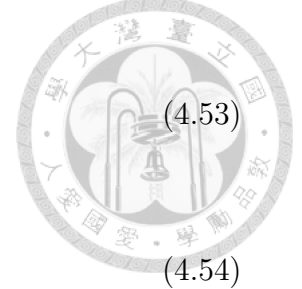
For both modulation schemes, the BER performance is greatly influenced by the received pattern of $c_0(t)$ and $c_1(t)$. In this section, $s_0(t)$ is set to be a pulse which represents RN releases 1000 molecules per second. It starts at $t = 0$ and with pulse width $w = 5 \text{ sec}$. In Fig. 24, different patterns of $c_0(t)$ are presented for different values of distance d and diffusion coefficient D . It can be observed that longer distance d results in lower concentration level, and also suppress components of $c_0(t)$ that lies in $[T_s/2, T_s)$, i.e., in $\text{supp}(c_0) \cap \text{supp}(c_1)$. In Fig. 25, $c_0(t)$ are plotted under different values of symbol interval T_s . When T_s is larger, components of $c_0(t)$ that lies in $[T_s/2, T_s)$ also become small. From (4.8) and (4.9), we define the signal to noise ratio (SNR) to be

$$\text{SNR} = \frac{c^2(t)}{\text{Var}(n_B(\mu, t))} \approx c(t), \quad (4.55)$$

when $p(t) \ll 1$.

4.4.1 Amplitude Modulation

For amplitude modulation, $s_0(t)$ is set to represents RN releases 1000 molecules per second which starts at $t = 0$ and with pulse width $w = 5 \text{ sec}$. The number of observations is $K = 10$. The relation between $s_0(t)$ and $s_1(t)$ is given in (4.20) with $C = 0.1$. In Fig. 26, BER performance is compared between the sample-based



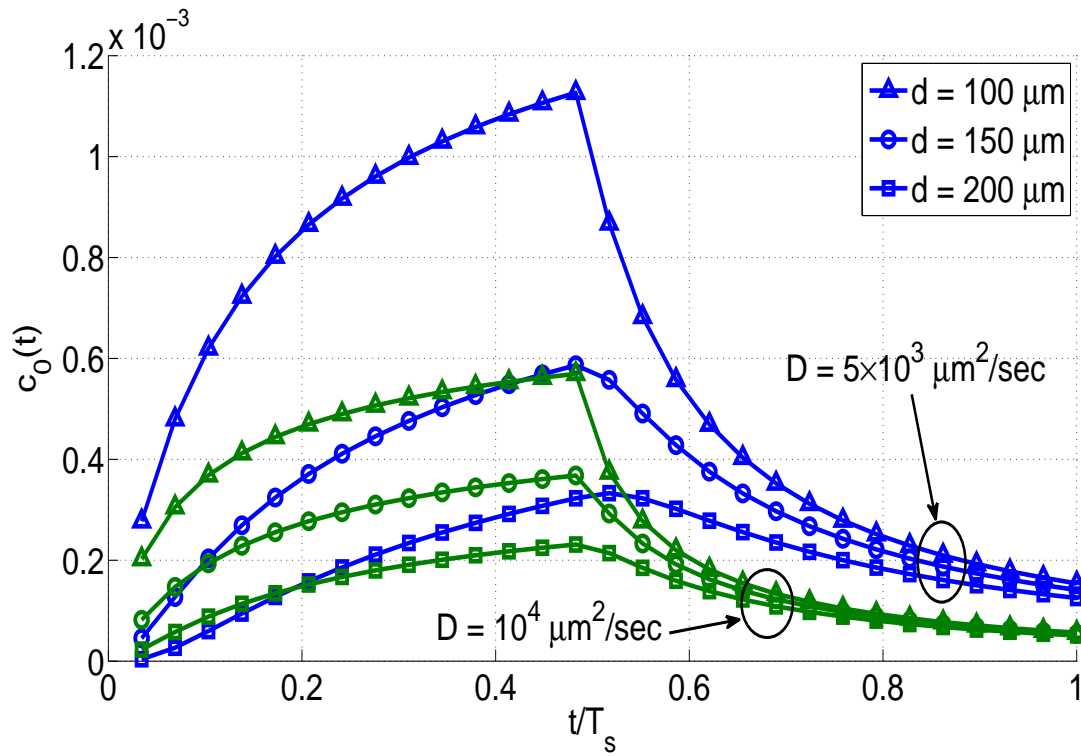


Figure 24: Patterns of the waveform $c_0(t)$ under different distance d and diffusion coefficient D . The time t is normalized with respect to T_s .

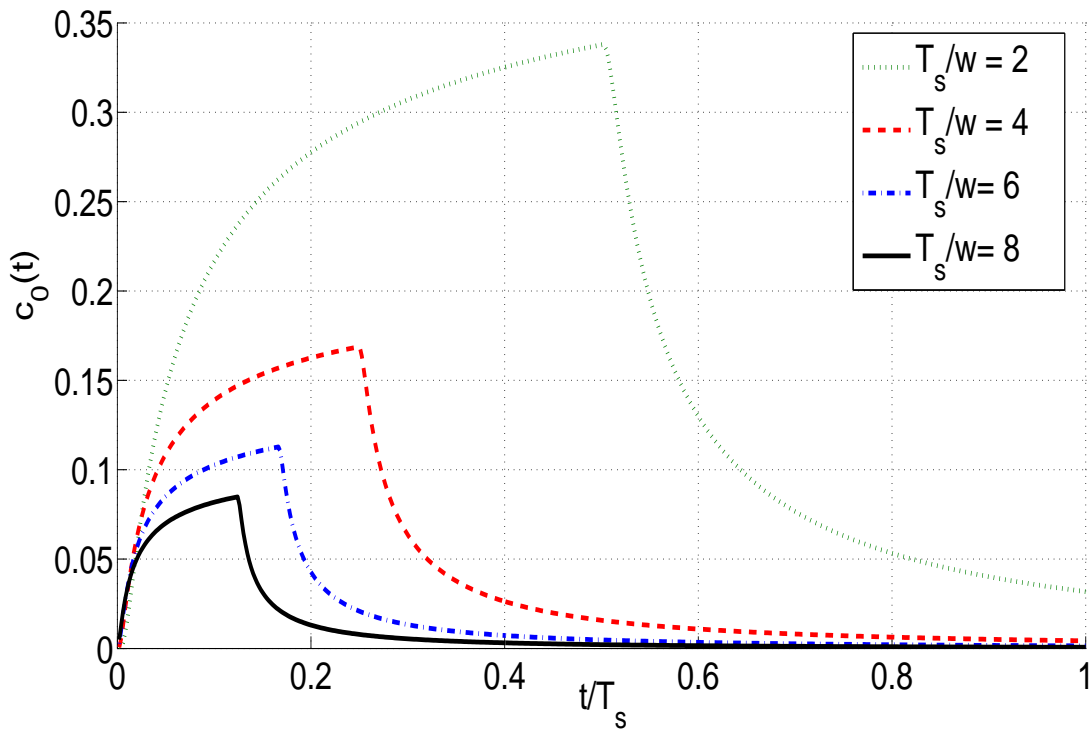


Figure 25: Patterns of the waveform $c_0(t)$ under different symbol duration T_s . The time t is normalized with respect to T_s .

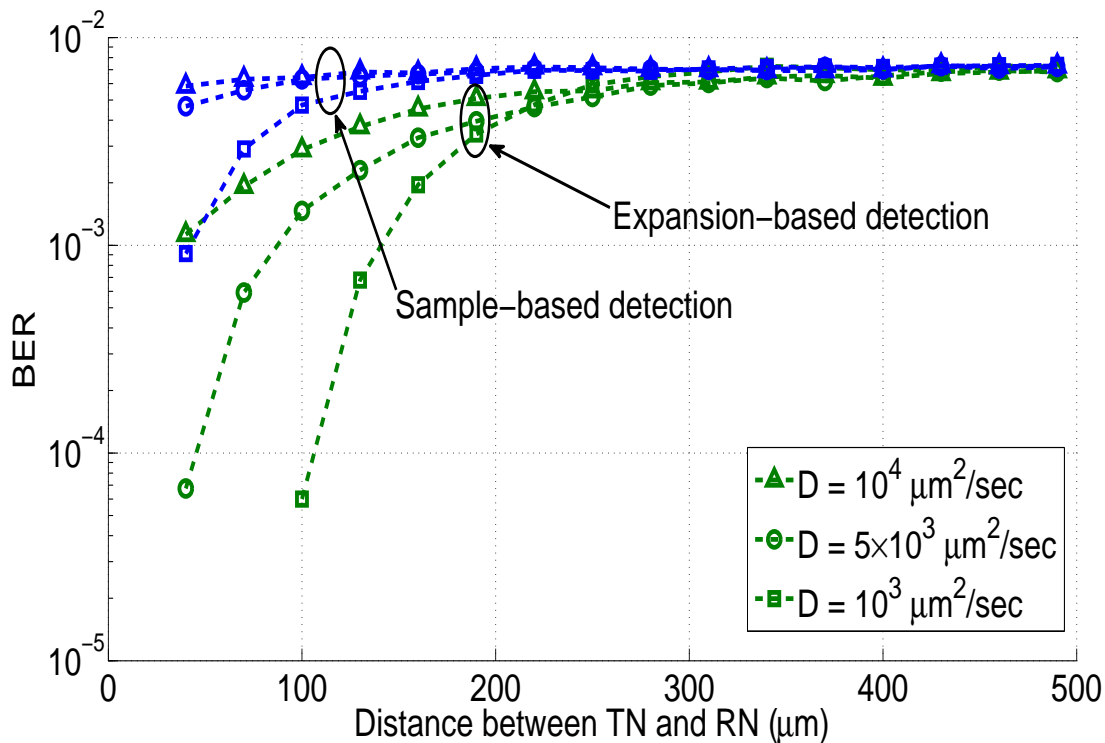


Figure 26: Comparison between the sample-based detection and the expansion-based detection for the amplitude modulation under different values of diffusion coefficient D .

detection and the expansion-based detection. The result shows that the BER increases when the diffusion coefficient D and the distance d between TN and RN become larger. This may be due to the larger SNR according to Fig. 24. Moreover, since $c_0(t)$ and $c_1(t)$ are multiple of each other for the amplitude modulation, BER performance can be roughly compared through the SNR. The figure also shows that when the distance between TN and RN is small, the expansion-based detection outperforms the sample-based detection very much. However, when the distance becomes larger, BER increases and the difference between two detection methods is not obvious. In Fig. 27, two detection methods are compared by different numbers of observations. The result quite matches the intuition that better performance can be achieved by having more observations on the received waveform, which is not only because more information about the waveform is available, but also the approximation in (4.43) is more accurate.

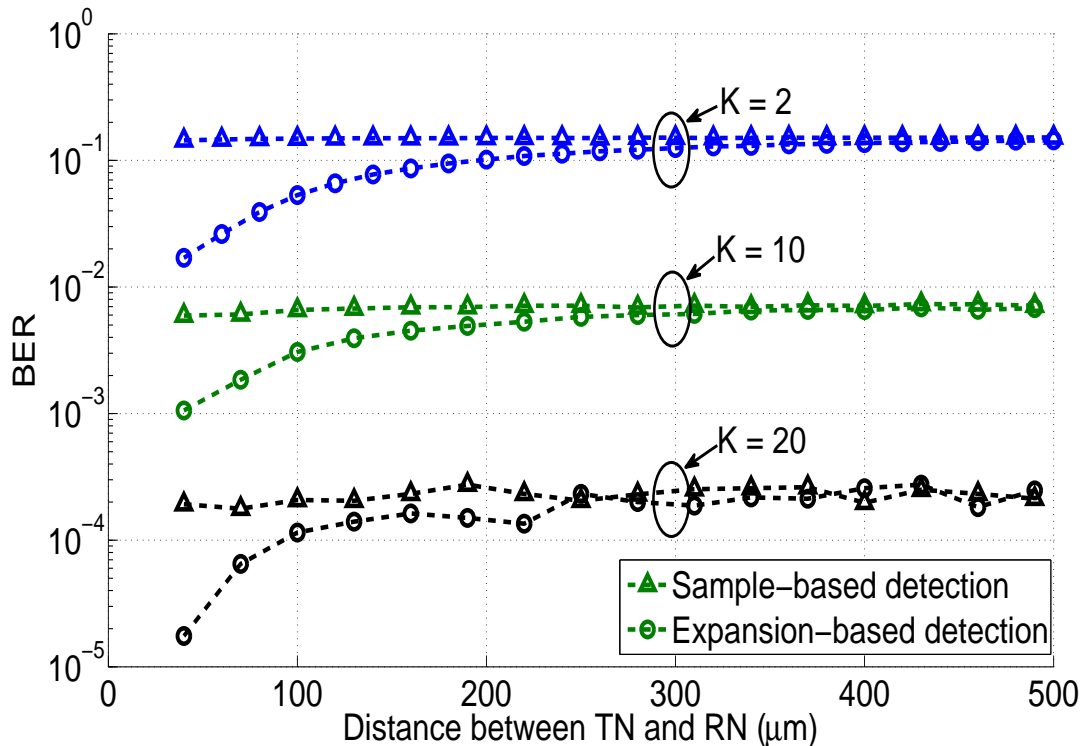


Figure 27: Comparison between the sample-based detection and the expansion-based detection for amplitude modulation under different number of observations K .

4.4.2 Pulse-position Modulation

For pulse-position modulation, the results of both detections are greatly influenced by how $c_0(t)$ and $c_1(t)$ occupies the time domain. In this part, $s_1(t)$ is obtained by right-shifting $s_0(t)$ for $T_s/2$, and hence it occupies $[T_s/2, T_s)$. Note that transmitting $s_1(t)$ in pulse-position modulation do not produce any error for one-shot transmission since RN can detect bit ‘1’ whenever a non-zero component is sensed in $[T_s/2, T_s)$. In this case, we only consider transmitting $s_0(t)$ and evaluate BER in terms of false-alarm probability, i.e., the probability that given TN transmitted bit ‘0’ but RN detects bit ‘1’. Fig. 28 compares two detection methods for pulse-position modulation by different values of diffusion coefficient. Unlike the amplitude modulation, BER performance of the pulse-position modulation becomes better for longer distance. And the relation between BER and diffusion coefficient D is not as straightforward as for the amplitude modulation. When d is small, a smaller value of D may perform worse than a larger value of

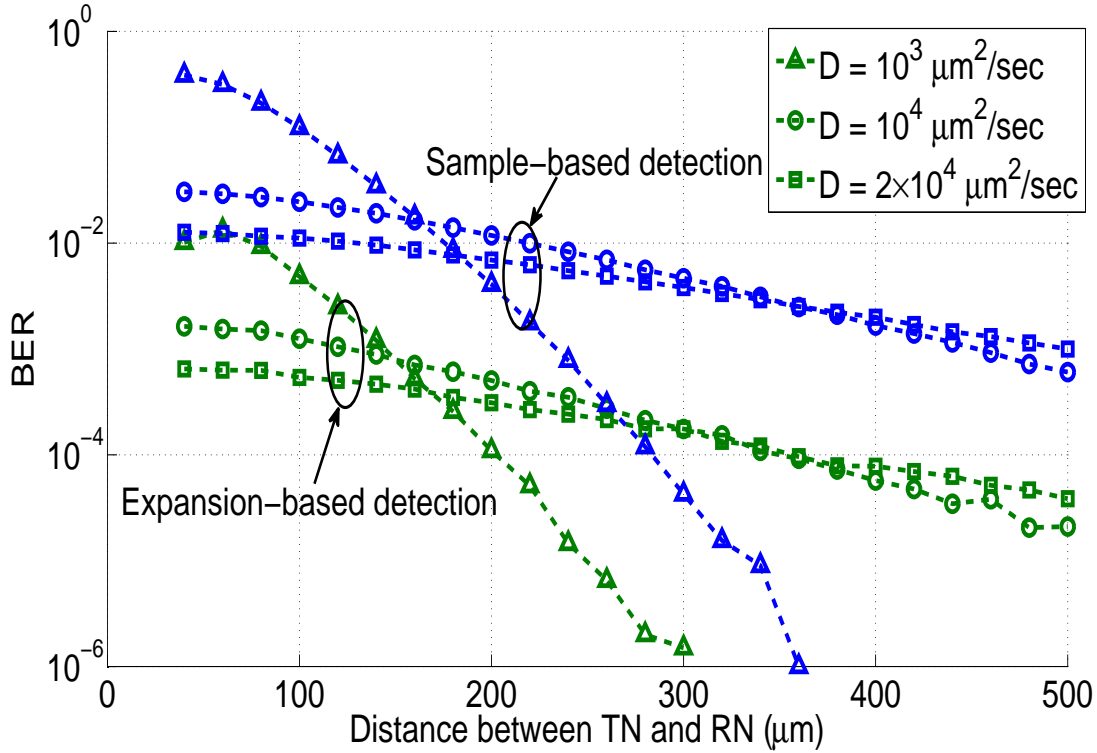


Figure 28: Comparison between the sample-based detection and the expansion-based detection for pulse-position modulation under different values of diffusion coefficient D .

D since components of $c_0(t)$ in the interval $[T_s/2, T_s)$ causes larger interference.

Fig. 29 compares BER for both detection methods under different numbers of observations K . For a fixed K , the expansion-based detection outperforms the sample-based detection. In Fig. 30, we vary the pulse width w of $s_0(t)$ and the result shows that larger values of T_s/w is beneficial to decrease the BER. As shown in Fig. 25, larger T_s/w indicates smaller interference from $c_0(t)$ to $c_1(t)$, which reduces the probability for false alarms to occur.

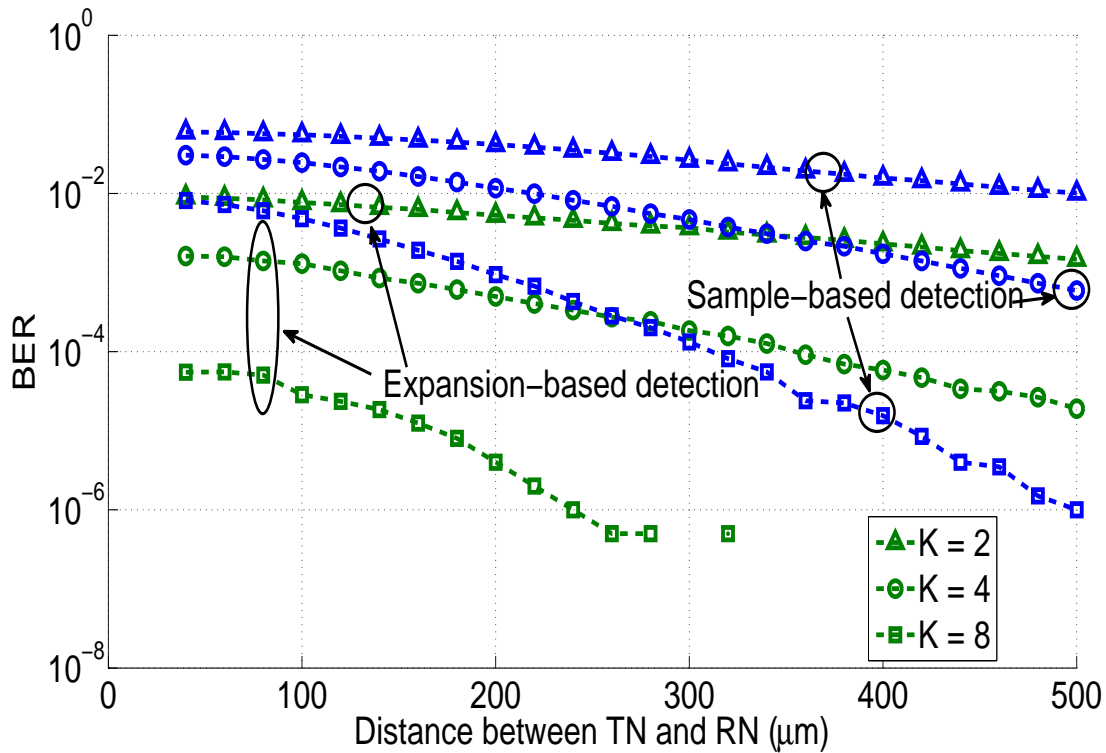


Figure 29: Comparison between the sample-based detection and the expansion-based detection for pulse-position modulation under different numbers of observations K .

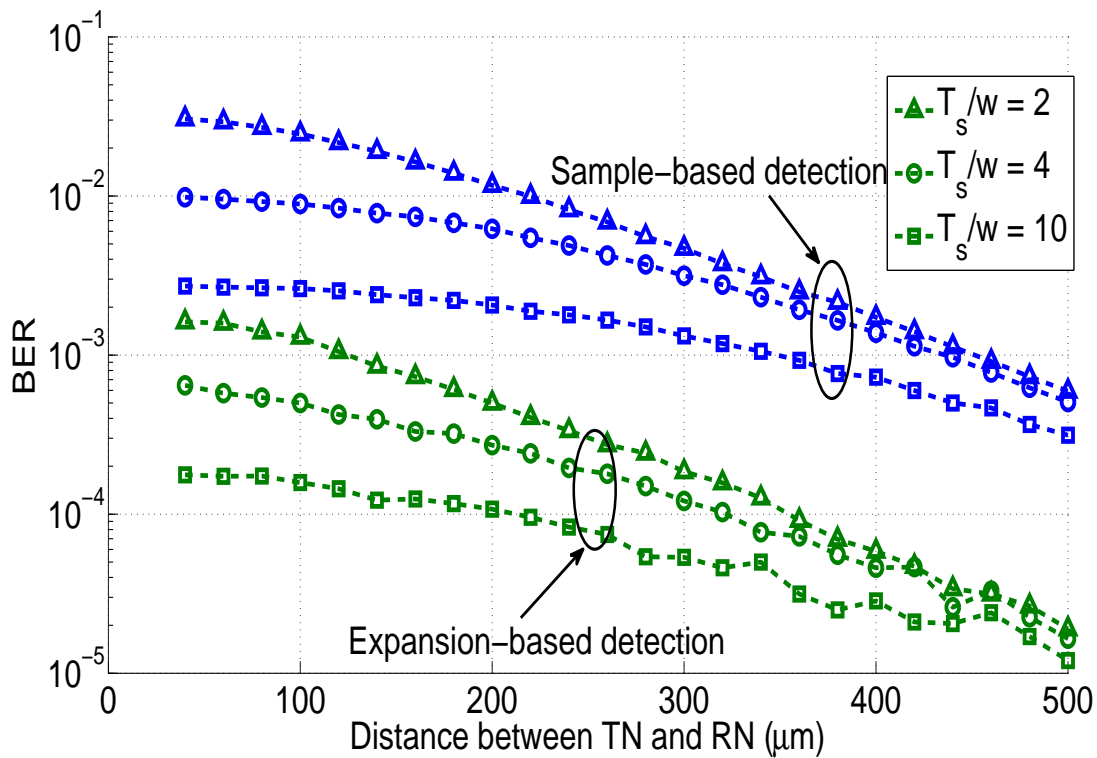


Figure 30: Comparison between the sample-based detection and the expansion-based detection for pulse-position modulation under different values of pulse width w .

CHAPTER 5



CONCLUSIONS AND FUTURE WORKS

5.1 *Conclusions*

In this thesis, two categories of molecular communication: coherent molecular communication and non-coherent molecular communication have been investigated. For coherent molecular communication, the channel behavior was described in a microscopic view, and the system design mainly focused on mitigating problems such as the crossover effect and the inter-symbol interference result from the random movements of molecules. Solutions to the problems were provided in Chapter 2 and Chapter 3. For non-coherent molecular communication, instead of treating each molecule independently, we tried to model the macroscopic behavior, that is, concentration level, for a large amount of molecules. Based on the model, signals could be modulated by different continuous waveforms at TN, and detected with low error rate at RN. The main achievements were discussed in previous chapters. In the following, we briefly summarize the contents of each chapter.

In Chapter 2, a quantity-modulated molecular communication system have been proposed. Based on the likelihood ratio test and Bayesian criterion, we obtained a low-complexity detection method. Moreover, we have explored series transmission with ISI. Numerical results have shown that by performing the proposed ISI cancellation, the performance improves significantly and the improvements becomes greater when more molecules are allowed to transmit a symbol.

In Chapter 3, a threshold-based detection algorithm have been proposed for the quantity-type-modulated system, and was proven to have good BER performance. Theoretical approximations have been derived for the BER performance of the threshold-based detection algorithm, and they match the simulation results well.

Finally, principles in choosing proper symbol duration, block length, and detection threshold were also presented, which enables a reliable molecular communication design.

In Chapter 4, a generalized stochastic model of the diffusion channel has been derived, which could be used to obtain the channel response when a continuous wave was transmitted. The proposed model enabled modulating information in different waveform of molecule releasing rate. Based on mathematical analyses, the expansion-based detection was proposed for amplitude modulation and pulse-position modulation. Simulation results have shown that the expansion-based detection out-performs the widely-used sampling-based detection. Moreover, from the simulation results, we concluded that the pulse-position modulation is preferred over amplitude modulation when the transmission distance is long.

5.2 *Future Works*

In this thesis, we consider one-dimensional environment for coherent molecular communication due to the fact that the distribution of the molecule first-hitting time in higher dimensional space is hard to evaluate. However, detection methods in three dimensional environment is still required in order to let the system physically realizable. It is served as our future work that the detection algorithm can be based on statistic of molecules, e.g. moments of the first-hitting time, without knowing the distribution of the first-hitting time.

For non-coherent molecular communication, we have found amplitude modulation and pulse-position modulation that can achieve simultaneous orthogonal expansion. It is of our interests to find either (1) a mathematically generalizable method to solve a set of basis functions for arbitrary continuous waveform or (2) other types of continuous waveform which can achieve simultaneous orthogonal expansion.

REFERENCES



- [1] N. Agoulmine, K. Kim, S. Kim, T. Rim, J.-S. Lee, and M. Meyyappan, "Enabling communication and cooperation in bio-nanosensor networks: toward innovative healthcare solutions," *IEEE Wireless Communications*, vol. 19, no. 5, pp. 42–51, October 2012.
- [2] T. Suda, T. Nakano, M. Moore, and K. Fujii, "Biologically inspired approaches to network systems," *Grid Enabled Remote Instrumentation*, pp. 99–113, 2009.
- [3] I. F. Akyildiz, F. Brunetti, and C. Blázquez, "Nanonetworks: A new communication paradigm," *Computer Networks (Elsevier) Journal*, vol. 52, no. 12, pp. 2260–2279, August 2008.
- [4] S. Hiyama, Y. Moritani, T. Suda, R. Egashira, A. Enomoto, M. Moore, and T. Nakano, "Molecular communication," in *Proc. 2005 NSTI Nanotechnology Conference*, May 2005, pp. 391–394.
- [5] P.-C. Yeh, K.-C. Chen, Y.-C. Lee, L.-S. Meng, P.-J. Shih, P.-Y. Ko, W.-A. Lin, and C.-H. Lee, "A new frontier of wireless communications theory: Diffusion-based molecular communications," *IEEE Wireless Communications Magazine*, vol. 19, no. 5, pp. 28–35, October 2012.
- [6] I. Llatser, A. Cabellos-Aparicio, and E. Alarcon, "Networking challenges and principles in diffusion-based molecular communication," *IEEE Wireless Communications*, vol. 19, no. 5, pp. 36–41, October 2012.
- [7] I. F. Akyildiz, F. Fekri, R. Sivakumar, C. Forest, and B. Hammer, "MoNaCo: fundamentals of molecular nano-communication networks," *IEEE Wireless Communications*, vol. 19, no. 5, pp. 12–18, October 2012.
- [8] S. Kadloor, R. Adve, and A. Eckford, "Molecular communication using brownian motion with drift," *IEEE Transactions on NanoBioscience*, vol. 11, no. 2, pp. 89–99, June 2012.
- [9] M. Pierobon and I. Akyildiz, "Diffusion-based noise analysis for molecular communication in nanonetworks," *IEEE Transactions on Signal Processing*, vol. 59, no. 6, pp. 2532–2547, June 2011.
- [10] M. U. Mahfuz, D. Makrakis, and H. T. Mouftah, "A generalized strength-based signal detection model for concentration-encoded molecular communication," in *Proceedings of the 8th International Conference on Body Area Networks*, 2013, pp. 461–467.
- [11] M. Kuran, H. Yilmaz, T. Tugcu, and I. Akyildiz, "Modulation techniques for communication via diffusion in nanonetworks," in *2011 IEEE International Conference on Communications (ICC)*, June 2011, pp. 1–5.

- [12] H. Shahmohammadian, G. G. Messier, and S. Magierowski, "Optimum receiver for molecule shift keying modulation in diffusion-based molecular communication channels," *Nano Communication Networks*, vol. 3, no. 3, pp. 183–195, 2012.
- [13] A. Eckford, "Nanoscale communication with brownian motion," in *2007 41st Annual Conference on Information Sciences and Systems (CISS)*, March 2007, pp. 160–165.
- [14] M. U. Mahfuz, D. Makrakis, and H. T. Mouftah, "Characterization of intersymbol interference in concentration-encoded unicast molecular communication," in *2011 24th Canadian Conference on Electrical and Computer Engineering (CCECE)*, May 2011, pp. 164–168.
- [15] L. Cui and A. Eckford, "The delay selector channel: Definition and capacity bounds," in *2011 12th Canadian Workshop on Information Theory (CWIT)*, May 2011, pp. 15 – 18.
- [16] J. G. Proakis and M. Salehi, *Communication Systems Engineering*. 5F, No.147, Chung-Ching South Road, Sec.1, Taipei, 10045, Taiwan, R.O.C.: Pearson Education Taiwan Ltd., 2010.
- [17] M. Haller, C. Heinemann, and R. H. Chow, "Comparison of secretory responses as measured by membrane capacitance and by amperometry," *Biophysical Journal*, vol. 74, pp. 2100–2113, April 1998.
- [18] R. S. Chhikara and J. L. Folks, *The inverse gaussian distribution: theory, methodology, and applications*. New York, NY, USA: Marcel Dekker, Inc., 1989.
- [19] L.-S. Meng, P.-C. Yeh, K.-C. Chen, and I. Akyildiz, "A diffusion-based binary digital communication system," in *2012 IEEE International Conference on Communications (ICC)*, June 2012, pp. 4985–4989.
- [20] H. L. V. Trees, *Detection, Estimation, and Modulation Theory – Part I*. John Wiley and Sons, Inc., 1968.
- [21] V. H. Poor, *An Introduction to Signal Detection and Estimation*. Springer-Verlag, 1998.
- [22] W.-A. Lin, Y.-C. Lee, P.-C. Yeh, and C.-H. Lee, "Signal detection and ISI cancellation for quantity-based amplitude modulation in diffusion-based molecular communications," in *Proc. IEEE GLOBECOM*, December 2012, pp. 4362–4367.
- [23] A. Eckford, "Achievable information rates for molecular communication with distinct molecules," in *2007 2nd BIONETICS*, December 2007, pp. 313–315.
- [24] Y.-P. Hsieh, P.-J. Shih, Y.-C. Lee, P.-C. Yeh, and K.-C. Chen, "An asynchronous communication scheme for molecular communication," in *2012 IEEE International Conference on Communications (ICC)*, 2012, pp. 6177–6182.

- [25] N.-R. Kim and C.-B. Chae, “Novel modulation techniques using isomers as messenger molecules for nano communication networks via diffusion,” *IEEE Journal on Selected Areas in Communications*, vol. 31, no. 12, pp. 847–856, December 2013.
- [26] —, “Novel modulation techniques using isomers as messenger molecules for nano communication networks via diffusion,” *IEEE Journal on Selected Areas in Communications*, vol. 31, no. 12, pp. 847–856, December 2013.
- [27] P.-J. Shih, C.-H. Lee, and P.-C. Yeh, “Channel codes for mitigating inter-symbol interference in diffusion-based molecular communications,” in *2012 IEEE Global Communications Conference (GLOBECOM)*, December 2012, pp. 4228–4232.
- [28] T. Kadota, “Simultaneously orthogonal expansion of two stationary gaussian processes examples,” *Bell System Technical Journal*, vol. 45, pp. 1071–1096, September 1966.
- [29] A. Hansson and T. M. Aulin, “On antenna array receiver principles for space-time-selective rayleigh fading channels,” *IEEE Transactions on Communications*, vol. 48, no. 4, pp. 648–657, April 2000.
- [30] P. Hansen, “Computation of the singular value expansion,” *Computing*, vol. 40, pp. 185–199, September 1988.